1

Models and Mechanisms of Cytochrome P450 Action

John T. Groves

1. Introduction

The reactions catalyzed by the cytochrome P450 family of enzymes have challenged and intrigued chemists for more than three decades. Alkane hydroxylation and olefin epoxidation, particularly, have attracted a sustained worldwide effort, the allure deriving both from a desire to understand the details of biological oxygen activation and transfer and, as well as the sense that the development of new, selective catalysts, based on these principles could be of considerable economic value. The focus of this chapter is on the advances in our understanding of the mechanisms of the remarkable oxygenation reactions mediated by oxometalloporphyrins in both enzymatic and in small molecule model systems. Particular emphasis is on the period since the publication of second edition of this monograph in 1995.

The activation and transfer of molecular oxygen into its substrate by an iron-containing enzyme was first demonstrated by Hayaishi in the 1950s[1]. It was shown, in some of the first mechanistically informative oxygen isotopic measurements, that both the inserted oxygen atoms in the conversion of catechol to *cis*-muconic acid derived from O_2 and not water. These findings challenged the then firmly held view that oxygen in biological molecules was derived exclusively from water via hydration processes. The biosynthesis of cholesterol and its precursor, lanosterol, from the hydrocarbon squalene were also shown to derive their oxygen functionality from molecular oxygen[2]. Here, a single oxygen atom derived from molecular oxygen while the other was transformed to water. Later, the prostaglandins were shown to derive from the incorporation of two molecules of oxygen to form, initially, an alkyl hydroperoxide-endoperoxide. Thus, what appeared at first to be an obscure process of bacteria and fungi became recognized as a major theme of aerobic metabolism in higher plants and animals. The subsequent search for "active oxygen species" and efforts to elucidate and understand the molecular mechanisms of oxygen activation and transfer have been richly rewarding. Novel and unusual iron redox chemistry, particularly those of high-valent metal–oxo and metal–peroxo species, has appeared as our understanding of enzymatic oxidation strategies has developed.

2. Oxygen Activation by Heme-Thiolate Proteins

The heme-containing metalloenzymes cytochrome P450[3], chloroperoxidase (CPO)[4, 5], nitric oxide synthase (NOS)[6], and their relatives catalyze a host of crucial biological oxidation reactions. Highly specific P450s are involved in the selective oxygenations of steroid and prostaglandin biosynthesis. Myeloperoxidase, which is a CPO, is an

John T. Groves • Department of Chemistry, Princeton University, Princeton, NJ.

Cytochrome P450: Structure, Mechanism, and Biochemistry, 3e, edited by Paul R. Ortiz de Montellano
Kluwer Academic / Plenum Publishers, New York, 2005.

integral part of the immune response, and NOS is the source of the highly regulated signal transducer, nitric oxide (NO). Certain fungal CPOs and bacterial P450s have been genetically engineered for large-scale biotransformations[7–10]. The active sites of these three protein families, known in detail from a number of X-ray crystal structures[4, 11–13], are remarkably similar. All three have an iron protoporphyrin IX center coordinated to a cysteine thiolate. All of them are oxidoreductases that activate molecular oxygen (O_2), in the cases of P450 and NOS, or hydrogen peroxide in the case of CPO, at the iron center and incorporate one of the oxygen atoms into a wide variety of biological substrates. The other oxygen atom is transformed into H_2O. All three proteins are proposed to initiate their chemistry through the oxidation of a resting iron(III) state (**1**) to a reactive oxoiron(IV) porphyrin cation radical intermediate (**2**) (Figure 1.1). A depiction of the CPO active site derived from the crystal structure of this protein from *Caldariomyces fumago* is shown in Figure 1.2. The structure, biochemistry, molecular biology, and the chemistry of cytochrome P450 and related model systems have been extensively reviewed [14–22].

Our understanding of the mechanism of action of these heme proteins comes from the direct

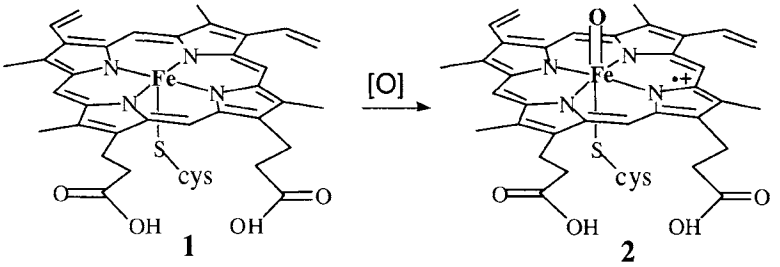

Figure 1.1. Iron(III) protoporphyrin IX with a cysteinate as the axial ligand (**1**), which is typical of cytochrome P450, chloroperoxidase (CPO), and nitric oxide synthase (NOS) enzymes. The active oxygen species of these proteins and related heme enzymes is an oxoiron(IV) porphyrin cation radical (**2**), often called compound I.

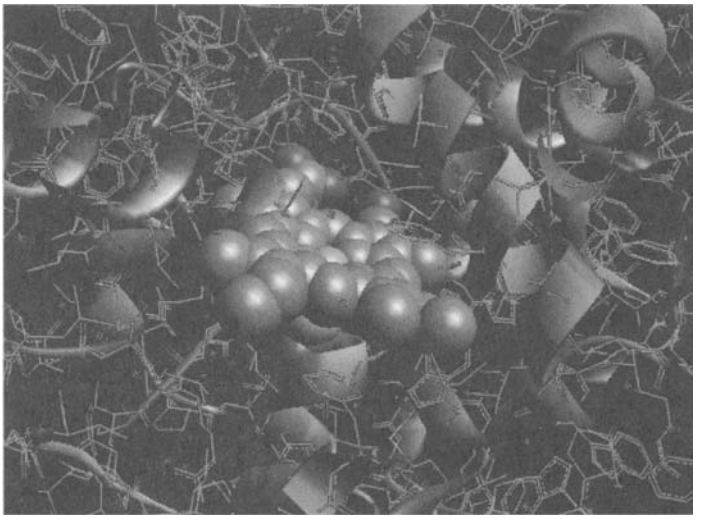

Figure 1.2. Crystal structure of the active site of chloroperoxidase (CPO) (EC 1.11.1.10) from *C. fumago*. Protein framework is shown as ribbons. The heme is buried in a hydrophobic binding pocket containing the iron-coordinating cysteinate ligand. Adapted from the X-ray atomic coordinates of CPO[4].

observation of intermediates in the catalytic cycle through a variety of spectroscopic techniques, the use of diagnostic substrates with mechanistically revealing rearrangements during oxidation, and the parallel development of the chemistry of synthetic metalloporphyrins. The principal features of the consensus mechanism of cytochrome P450[23] are as outlined in Scheme 1.1:

(1) binding of substrate to the enzyme, sometimes accompanied by a spin-state change of the iron, to afford an enzyme–substrate adduct **3**;
(2) reduction of the ferric cytochrome P450 by an associated reductase with an NADPH-derived electron to the ferrous cytochrome P450 **4**;
(3) binding of molecular oxygen to the ferrous heme to produce a ferrous cytochrome P450–dioxygen complex **5**, similar to the situation in oxymyoglobin;
(4) a second one-electron reduction and protonation to arrive at the Fe(III)–hydroperoxy complex **6**;
(5) protonation and heterolytic cleavage of the O–O bond in **6** with concurrent production of a water molecule to form a reactive iron–oxo intermediate **7**;
(6) and, finally, oxygen-atom transfer from this iron–oxo complex **7** to the bound substrate to form the oxygenated product complex **8**. Product dissociation completes the cycle.

There were a number of important realizations in the course of elucidating this mechanism. That hydrogen peroxide, alkyl hydroperoxides, peroxyacids, periodate, and iodosylbenzene were also functional with cytochrome P450 suggested that the chemistry of "oxygen activation" was the two-electron reduction of molecular oxygen to hydrogen peroxide and that, in analogy to the peroxidases, the active oxygen species was a ferryl (or oxene) complex Fe=O, formally iron(V). It was shown that a synthetic oxoiron(IV) porphyrin cation radical species could be formed at low temperature by the oxidation of an iron(III) precursor with peroxyacids (**9** → **10**)[24]. Intermediate **10** did have the requisite reactivity to transfer an oxygen atom to hydrocarbon substrates. It is this oxygen-atom transfer from

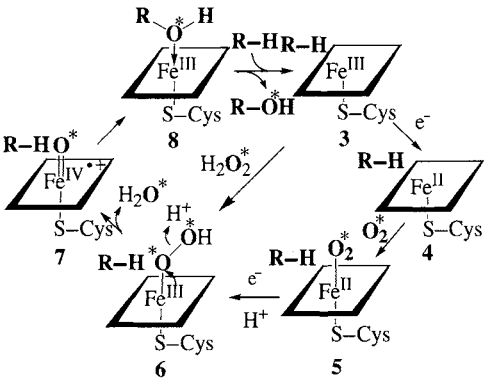

Scheme 1.1. Consensus catalytic cycle for oxygen activation and transfer by cytochrome P450.

the oxygen donor to form the Fe=O intermediate **7** and the subsequent oxygen transfer to form the substrate complex **8** that has been termed *oxygen rebound*[25]. Such an iron–oxo species (compound I) has been observed for the CPO of *C. fumago*[26] but the active species of cytochrome P450 has remained elusive. Very recently, it has been shown that an intermediate with the spectral properties similar to those of CPO compound I and the model iron porphyrin systems is formed upon the oxidation of Cyp119, a thermostable cytochrome P450, with a peroxyacid, analogous to the model systems[27]. Consistent with the high reactivity expected for P450 compound I, this intermediate decayed with a rate constant of 29 s^{-1} at 4°C. Interestingly, similar experiments with $P450_{cam}$, the camphor-oxidizing enzyme from *Pseudomonas putida*, resulted in an iron(IV)–protein tyrosine radical species, presumably via a one-electron oxidation of Tyr96 which is only 9.4 Å from the iron center[26].

3. Mechanism of Hydroxylation by Cytochrome P450

There has been much discussion in the field about the oxygen transfer process **6** → **7** → **8**. The oxygen rebound mechanism in Scheme 1.1 is consistent with the stereochemical, regiochemical, and allylic scrambling results observed in the oxidation of norbornane, camphor, and cyclohexene by cytochrome P450. The hydroxylation of

a saturated methylene (CH_2) in norbornane was accompanied by a significant amount of epimerization at the carbon center[25]. Thus, the hydroxylation of *exo-exo-exo-exo*-tetradeuterionorbornane by P450 2B1 and the hydroxylation of camphor by $P450_{cam}$[28] gave *exo*-alcohol with retention of the *exo*-deuterium label (Scheme 1.2). The hydroxylation of selectively deuterated cyclohexene proceeded with substantial allylic scrambling[29]. The intrinsic isotope effects for the oxygen insertion into a C–H bond are very large, in the range of 10–13.5. These large isotope effects are inconsistent with an insertion process and indicate that the C–H bond is essentially half-broken in a linear [O·H·C] transition state thus providing strong evidence for a nonconcerted mechanism. Significantly, model iron porphyrin systems displayed the same behavior for both the norbornane[30] and cyclohexene[29] substrates. Thus, one concludes that the epimerization and allylic scrambling processes are intrinsic properties of the oxygen transfer event from an oxoiron complex.

Another revealing probe of the nature of P450-mediated hydroxylation is a study of the

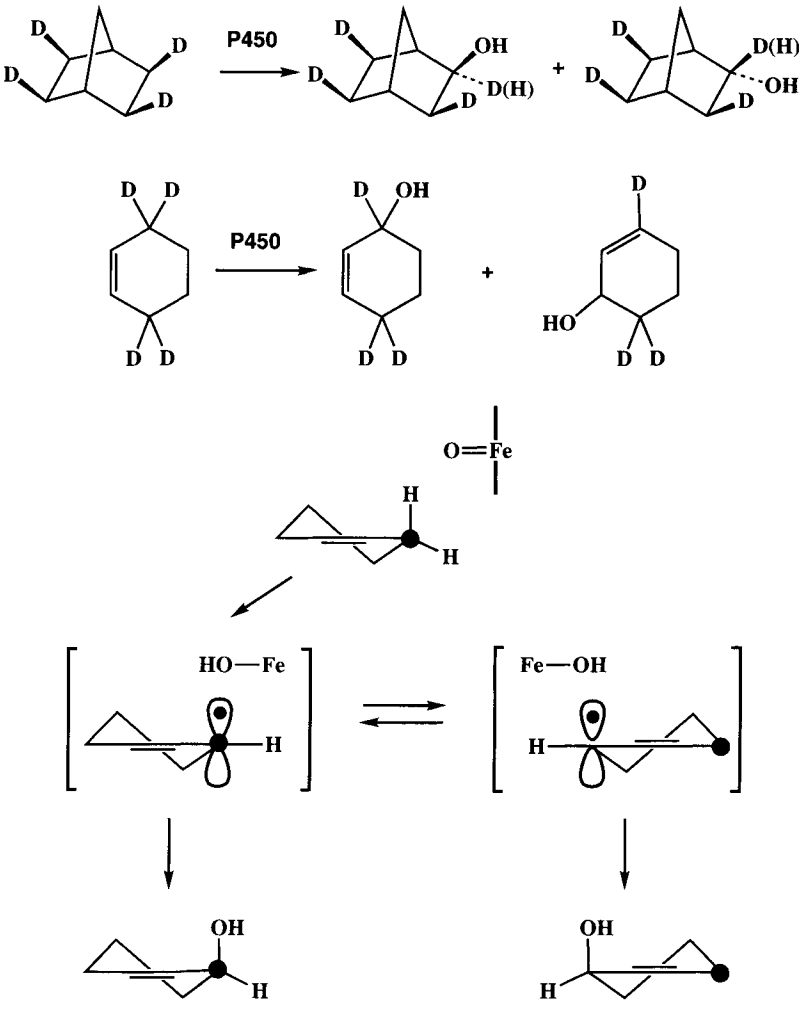

Scheme 1.2. Epimerization and allylic scrambling observed for cytochrome P450 catalyzed hydroxylation.

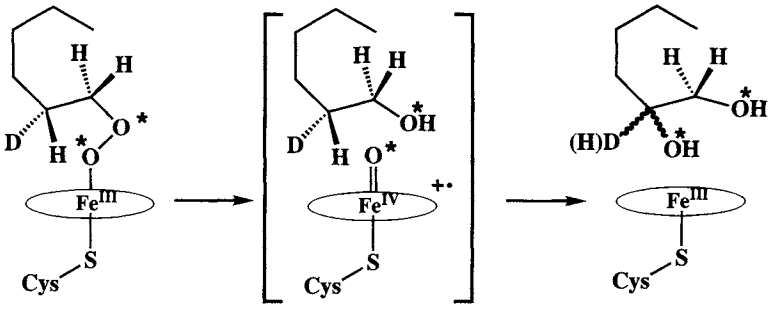

Scheme 1.3. Hydroperoxide isomerase activity of cytochrome P450 is intramolecular.

hydroperoxide isomerase activity of these enzymes. 1-Hydroperoxyhexane has been shown to afford 1,2-dihydroxyhexane upon exposure to P450 2B1[31]. This is an unusual reaction since the oxidizing equivalents of the hydroperoxide have been used in this case to hydroxylate the *neighboring* methylene group. A mixed, double oxygen label experiment established that the rearrangement was *intramolecular* (Scheme 1.3). Thus, the terminal hydroperoxide oxygen was incorporated into the adjacent C–H bond. This reaction pathway is pertinent to the discussion about the nature of reactive P450 intermediates since the same ferryl species (compound I) can be accessed by this "peroxide shunt" pathway. Analysis of the diols derived from chirally labeled 2-deuterio-1-hydroperoxyhexane showed that there was a loss of stereochemistry at the hydroxylated carbon center. Accordingly, the results support a mechanism involving initial peroxide heterolysis, hydrogen abstraction at the adjacent methylene, and radical recombination to afford the product diol. The result is revealing since O–O bond homolysis to form a hexyloxy radical should lead instead to γ-hydrogen abstraction and products derived therefrom.

Kupfer *et al.* have used this P450-hydroperoxide isomerase reaction to explore substrate mobility at the enzyme active site during the hydroxylation event[32]. Isomerase substrates were found to remain in proximity to the P450 oxoferryl intermediate and were rapidly captured by the oxidant with high efficiency. Monooxygenase substrates, by contrast, apparently bind to ferric P450 in multiple orientations and undergo more extensive substrate reorientation prior to oxidative attack. This difference is likely to be due to the requisite prepositioning of the hydroperoxide as a ligand of Fe(III). During turnover via oxygen reduction, however, the positioning of the substrate will be dictated by substrate–active-site interactions. An important conclusion from these studies is that product selectivity can be affected significantly by substrate mobility. Accordingly, *changes in product selectivity*, which have been used to suggest alternative oxidants, need to be interpreted with caution.

The hydroperoxy iron(III) complex **6** has also been suggested to effect substrate oxygenations based on observed changes in product ratios and loss of hydrogen peroxide (uncoupling) upon P450 active-site mutations[33–35]. An important recent advance has been the development of cryospectroscopic studies by Hoffman *et al.* that have allowed the stepwise interrogation of intermediates depicted in Scheme 1.1[36]. Thus, the injection of an electron into complex **5** via γ-radiation, followed by thermal annealing of the sample has produced EPR and ENDOR evidence for the formation of, first, a hydrogen bonded iron–peroxo species and then the iron–hydroperoxo complex **6**. While no ferryl intermediate **7** was observed, the product alcohol was found to be formed with its oxygen atom *coordinated to the iron center and with the substrate-derived proton attached to the product alcohol* as depicted in structure **8** (Scheme 1.1). This arrangement has important mechanistic implications since, if a ferryl species **7** were the immediate precursor of the product complex **8**, then coordination of the product hydroxyl oxygen would be a necessary consequence. By contrast, if

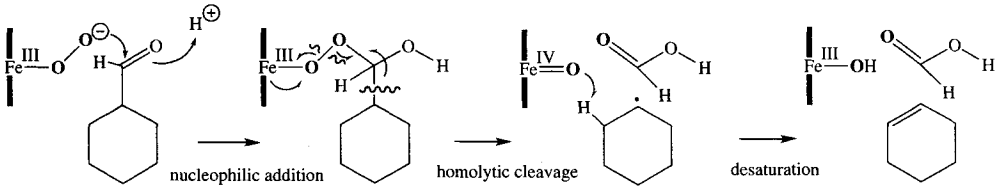

Scheme 1.4. Proposed mechanism for the deformylation typical of P450 aromatase activity.

the hydroperoxo species **6** were the source of the electrophilic oxygen, then *water* would be coordinated to iron rather than the product alcohol. A product complex such as **8** could also be the source of cationic rearrangement products that are sometimes observed during P450 oxygenations.

Significant recent advances in computational approaches to the study of biological catalysis, and the applications of these techniques to the cytochrome P450 mechanism have also been illuminating. Thus, Shaik *et al.*[37] and Yoshizawa *et al.*[38], have presented the results of a density functional theory (DFT) analysis of the reactivity of hydroperoxyiron(III) complexes such as **6**. Both groups conclude that a hydroperoxyiron(III) porphyrin, Fe(III)–OOH, would be an implausible primary oxidant. The protonation and heterolytic O–O bond cleavage of **6** to afford a ferryl species analogous to **7** was found to proceed with almost no energetic barrier, in accord with earlier experimental results for the oxidation of an iron(III) porphyrin **9** to an oxoiron(IV) porphyrin cation radical species **10** with a peroxyacid[39]. Further, the oxygen transfer from **7** to ethylene to form an epoxide proceeded with only a low barrier. It was concluded that the DFT calculations exclude a hydroperoxyiron(III) intermediate such as **6** as a reactive, electrophilic oxidant. Several modes of oxygen transfer from the hydroperoxide intermediate encountered exceedingly high barriers for reaction. The lowest energy of these was an interaction of the substrate ethylene with the *proximal*, iron-bound oxygen of the Fe(III)–OOH ensemble.

Nucleophilic reactions of a hydroperoxyiron(III) intermediate **6**, as have been suggested by Akhtar[40], Robinson[41], and Vaz and Coon[42], for the deformylation reactions characteristic of the P450 aromatase, do seem to be suggested by the significant basicity of the distal, hydroxylic oxygen found in the calculations for the Fe(III)–OOH group. This mode of reactivity is highly analogous to the reactions of enzymes such as cyclohexanone monooxygenase that proceed through a flavin 4a-hydroperoxide[43]. Here, only *electron-deficient* olefins react to afford epoxides even though the flavin hydroperoxide is 2×10^5 times more reactive than a simple alkyl hydroperoxide[44]. The reader is referred to an insightful review by Watanabe for a thorough discussion of the various modes of reactivity of peroxoFe(III) porphyrins (Scheme 1.4)[45].

The hydroxylation of a C–H bond does seem to require the full formation of a reactive ferryl intermediate as in **11**. This applies both for the reductive activation of dioxygen and for the very revealing cases of alkyl hydroperoxide isomerization catalyzed by P450 discussed above[31, 32]. For P450s in which the proton relay system has been disrupted by active-site mutations, one would expect that particularly reactive substrates could interact with the proximal oxygen earlier in this reaction profile as shown in **12**. While similar atomic trajectories and electronic charge redistributions are followed in each case, the former (**11**) is analogous to the S_N1 reaction in organic chemistry, generating a discrete ferryl intermediate, while the latter (**12**) is S_N2-like, requiring assistance from the electron-rich substrate. Indeed, in a recent report by Sligar and Dawson, mutation of the conserved active-site threonine-252 to alanine in $P450_{cam}$ was shown to disable camphor hydroxylation while maintaining some reactivity for more reactive olefinic substrates[46]. Similarly, two reactive intermediates, as suggested by Jones[47] for the reactions of a thioether substrate, and also for model porphyrin systems described by Nam[48], could reasonably derive from a mechanistic spectrum of this type. An important precedent for this behavior is seen in the reactions of peroxyacids with model Fe(III) porphyrins. Thus, Watanabe and Morishima have shown that the iron-coordinated peroxyacid **9** reacted with olefins at the *iron-coordinated oxygen atom* in nonpolar

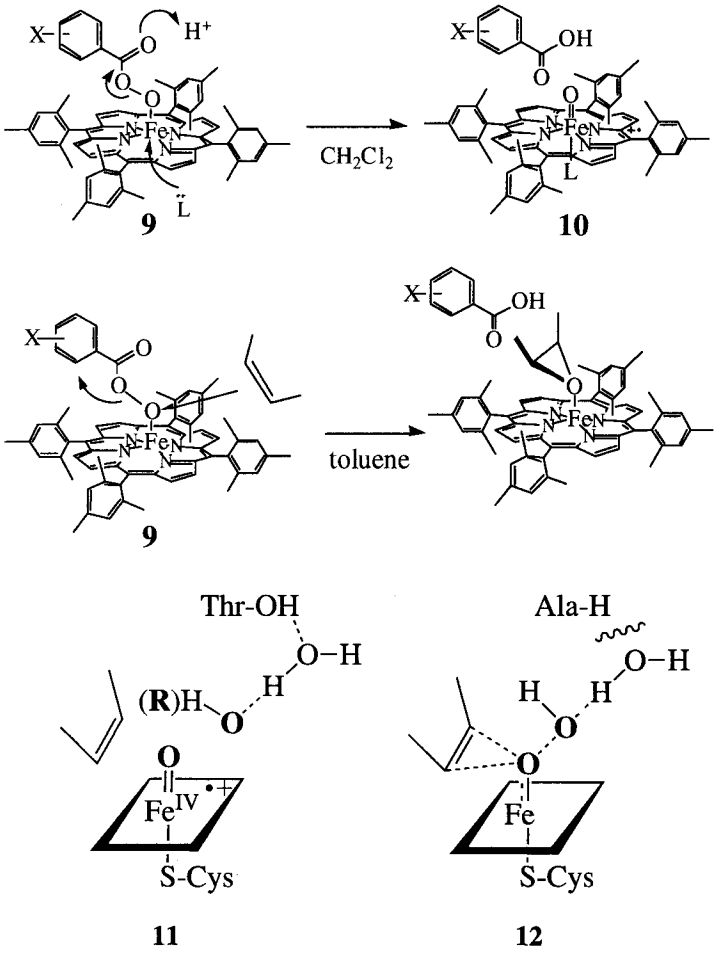

solvents to give epoxides but would not react with saturated hydrocarbons[45, 49]. By contrast, the same oxoiron(IV) porphyrin cation radical, **10**, was formed with a variety of peroxyacids in more polar media. This effect is also seen in model compounds with a thiolate ligand to iron[50]. The protein-derived hydrogen bonds to the axial thiolate ligand to iron in $P450_{cam}$ have been shown to affect the O–O bond cleavage[51].

4. Mechanisms and Molecular Trajectories for Hydroxylation by Cytochrome P450

Among all the varied reactions mediated by cytochrome P450, none has captured the imagination of chemists more than the hydroxylation of saturated carbon centers. Metal–oxo reagents such as chromates and permanganate can perform reactions of this type but are notoriously nonselective and must be used under forcing conditions. The selective hydroxylation of hydrocarbons remains one of the grand challenges for the chemical catalysis community. How can a protein create an iron intermediate reactive enough to hydroxylate even as inert a substrate as cyclohexane and not oxidize the relatively fragile protein superstructure? What is the electronic structure of that intermediate and what are the molecular pathways for oxygen insertion into a C–H bond? Without clear answers to these questions, the chemical catalysis performed by these metalloenzymes will remain an enigma and our

attempts to draw conclusions will be without physical meaning. Without knowledge of the mechanism, we learn nothing of predictive value that could be applied to other systems such as the rational design of enzyme inhibitors or the development of enzymatically inspired catalysts.

Presented in Scheme 1.5 is the range of mechanisms that have been considered as likely candidates for the cytochrome P450-catalyzed hydroxylation of hydrocarbons and those of model iron, manganese, and ruthenium porphyrins. A linear, *homolytic* transition state, as in intermediate **H**, best fits the available data, such as the very large hydrogen isotope effects. Indeed, extensive similarities to the hydrogen abstraction observed by cytochrome P450 and a *t*-butoxy radical have been presented by Dinnocenzo and Jones in support of this view[52]. A nonconcerted pathway for C–H bond cleavage is strongly supported by the observations of a variety of molecular rearrangements that are known to accompany P450-mediated hydroxylation as discussed above. Initially it was clear that the kinds of rearrangements observed were consistent with the formation of a caged substrate radical at the heme active site. The intermediate radical could be trapped in a subsequent step. Both P450 enzymes and model systems showed a nonstereospecificity for the hydrogen removal step from norbornane or camphor substrates. Such a process was counterindicative of a cationic pathway to explain the observed rearrangements. The results rule out *freely diffusing* radicals, but a short-lived substrate radical would explain the observed results.

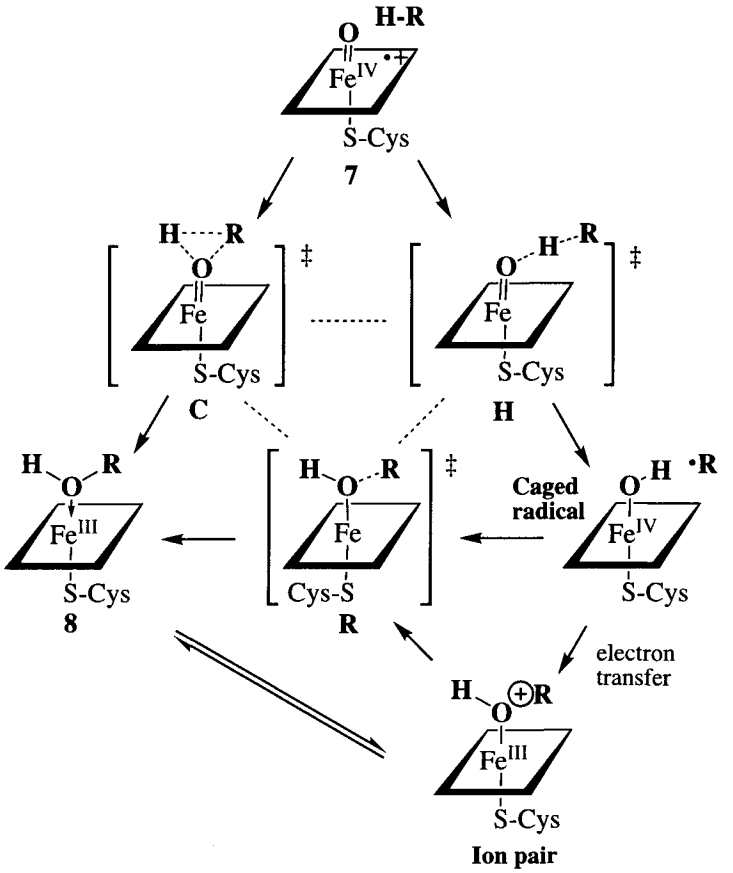

Scheme 1.5. Pathways for oxygen-atom transfer from the active ferryl species 7 of heme-thiolate enzymes such as cytochrome P450 to form the product alcohol coordinated to the ferric, resting form of the protein (**8**).

It was shown by Ortiz de Montellano *et al.* that bicyclo[2.1.0]pentane was oxidized by rat liver microsomes to a 7 : 1 mixture of *endo*-2-hydroxybicyclo[2.1.0]pentane and 3-cyclopenten-1-ol, consistent with a radical ring-opening reaction[53]. Applications of the "radical-clock" method by Ingold[54] and by Newcomb[55] began to measure the lifetime of the suspected radical cage intermediate. The rate constant for the rearrangement of bicyclo[2.1.0]pent-2-yl radical to 3-cyclopenten-1-yl radical was determined to be $2.4 \times 10^9\ s^{-1}$ at room temperature by using laser flash photolysis techniques[56]. Thus, a rate constant of $k_{OH} = 1.7 \times 10^{10}\ M^{-1}\ s^{-1}$ was estimated for the rebound process. Radical clocks with very fast rearrangement times were shown to produce *less* rearrangement than slower clocks in the P450-mediated hydroxylations, however. The results led Newcomb to question whether a radical pathway existed since the apparent lifetimes revealed by these probes were in the range of 100 fs, too short to represent a bona fide intermediate[57]. Several suggestions have been considered to resolve this dilemma and the question is still an area of active experiment and debate. As shown in Scheme 1.5, the transition state for hydrogen abstraction will position the active oxygen only a few tenths of an Angstrom *farther* from the hydroxylated carbon atom than the transition state for the ultimate C–O bond formation. Thus, the extent of radical rearrangement might be expected to depend critically on the *tightness* of the radical cage and the ensemble of steric and electronic forces experienced by the incipient radical within the cage. Even the molecular makeup of the active site will depend on how the substrate fills the site, leaving room for movement of amino acid side chains in the vicinity of the substrate or allowing additional water molecules into the active-site area. The extent of rearrangement detected by a particular probe may simply reflect a facile molecular trajectory from the hydrogen abstraction transition state to the hydroxylation transition state in this variable environment. For substrates with a very strong C–H bond and a small steric size, both effects would push the reaction coordinate toward a tighter radical cage.

Indeed, it has been shown that the effective *lifetime* of a radical intermediate can even be affected by the stereochemistry of the hydrogen abstraction event[23]. The chiral, binaphthyl porphyrin shown in Figure 1.3 has been found to hydroxylate ethylbenzene with a 70% *ee*. Stereoselective deuteration of the substrate revealed that the pro-*R* hydrogen of ethyl benzene was hydroxylated with nearly complete retention of configuration at carbon while the pro-*S* hydrogen underwent significant racemization (Figure 1.3). Interestingly, the partition ratio, retention/inversion, was nearly the same for the two enantiomers of ethylbenzene-d_1, suggesting similar mobility of the radical intermediate at the active site.

Evidence for a similar type of host–guest complementarity effect has been presented recently by Wüst for the hydroxylation of limonene by the limonene-6-hydroxylase, P450 CYP71D18[58]. The regiochemistry and facial stereochemistry of the limonene hydroxylation was found to be determined by the absolute configuration of the substrate. Thus, (−)-(4*S*)-limonene gave (−)-*trans*-carveol as the only product, whereas (+)-(4*R*)-limonene afforded mostly (+)-*cis*-carveol in a mixture of products. Specifically deuterated limonene enantiomers revealed that (4*R*)-limonene has sufficient freedom of motion within the active site of CYP71D18 to allow formation of either the *trans*-3- or *cis*-6-hydroxylated product. However, the kinetic isotope effects resulting from deuterium abstraction were significantly smaller than expected for an allylic hydroxylation. Significantly, the oxygenation of (4*R*)-limonene gave *trans*-carveol with considerable allylic rearrangement and stereochemical scrambling, while the formation of (+)-*cis*-carveol proceeded with high stereospecificity for C6 hydrogen abstraction and little rearrangement. These results are analogous to the ethylbenzene hydroxylation by the chiral iron porphyrin described above, in that epimerization and allylic rearrangement apparently depend upon the fit and mobility of the substrate at the active site. Another informative probe of substrate mobility at the active site using kinetic isotope effect has been presented by Jones and Trager[59].

For a reaction that involves a paramagnetic iron–oxo intermediate and proceeds to produce paramagnetic radical intermediates, it is likely that spin-orbit coupling effects and the spin states of reacting intermediates may offer another significant consideration[60]. Schwarz first suggested that the unusually slow reaction of FeO^+ with hydrogen in the gas phase was due to spin-conservation effects that were imposed on these

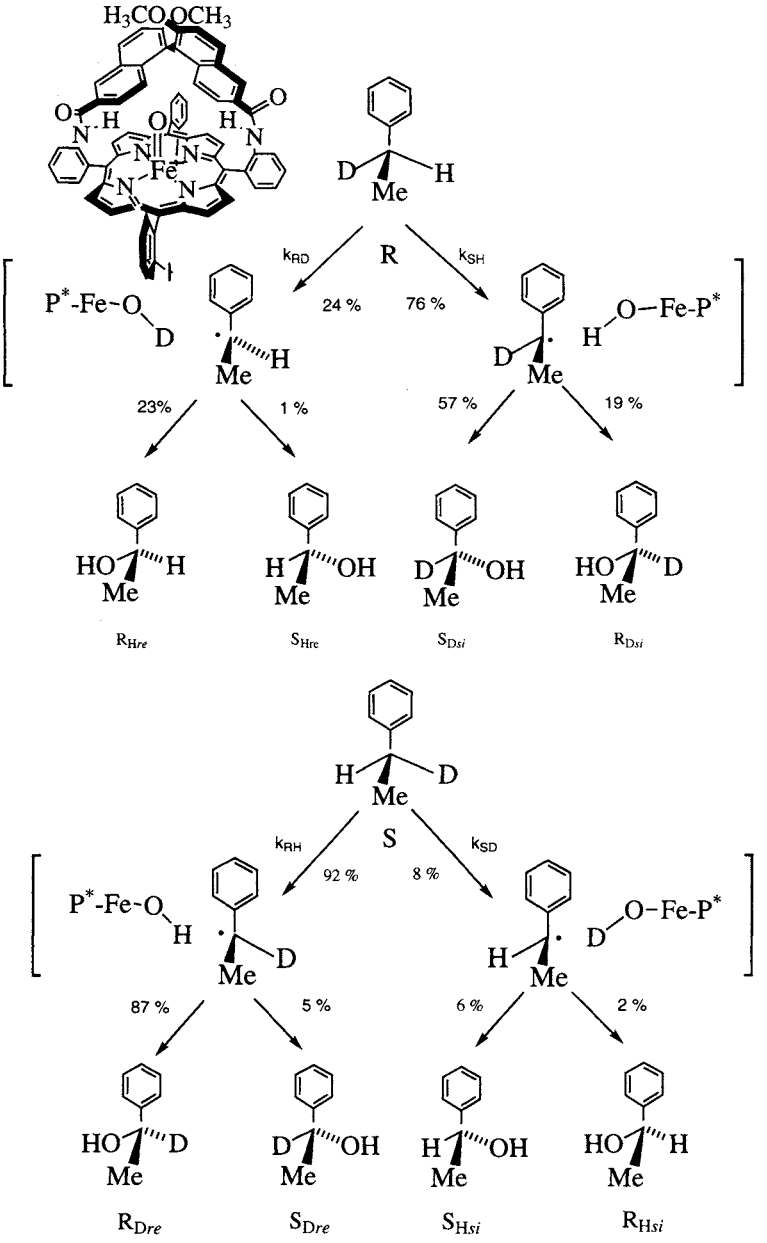

Figure 1.3. Catalyic asymmetric hydroxylation by a chiral, binaphthyl porphyrin. The stereochemical outcome of a hydroxylation depends upon the steric fit of the substrate.

intermolecular encounters[61]. Detailed DFT calculations on this simplest iron–oxo electrophile showed that there was a spin-state crossover during the H–H bond cleavage step to form a species H–Fe–OH^+, and another spin crossover leading to the product $Fe(OH_2)^+$. Thus, the lowest energy pathway for the reaction involved crossing from an initial high-spin, sextet state for the oxidant FeO^+ to a low-spin, quartet state near the transition state for H–H bond cleavage. While such effects are common for first-row elements as, for example, with singlet and triplet carbenes, "spin forbiddenness" has usually been discounted for reactions involving transition metals. However, the successful application of DFT calculations to explain the unusual behavior of FeO^+ suggests that these effects may be significant in the area of oxidative catalysis.

Shaik has applied these considerations to examine interactions of a prototype substrate, methane, with a ferryl intermediate similar to **7** to probe this chemistry of P450[62]. The results are very revealing. The ferryl intermediate was shown to have two nearly isoenergetic electron configurations, doublet and quartet, depending upon whether the unpaired electron in the porphyrin cation radical is ferromagnetically or antiferromagnetically coupled to the triplet ferryl center. Indeed, both situations are known in enzymatic compounds I and model systems. The calculations indicate that the transition state for C–H bond cleavage does look like the extended arrangement **H** in Scheme 1.5. Here, however, the molecular trajectories for the high-spin and low-spin reaction coordinates diverge. For the high-spin pathway, there was a discernable intermediate caged radical state with the carbon center interacting weakly with the iron–hydroxide. A significant energy barrier was found for collapse of this high-spin intermediate to the product via formation of a carbon–oxygen bond. By contrast, the low-spin trajectory could proceed to products without encountering this barrier. This two-state hypothesis could provide a way out of the mechanistic dilemma presented by the radical clock results since the apparent timing of the clocks would depend upon the relative importance of the high- and low-spin pathways that would likely vary from substrate to substrate.

Evidence for short-lived substrate radicals has been presented recently for the oxidation of the mechanistically diagnostic probe molecule norcarane by cytochrome P450[63]. Among the products found with P450 BM3, was 1.3% of the radical rearrangement product hydroxymethylcyclohexene while the cation rearrangement product 3-cycloheptenol was not observed with that isozyme (Figure 1.4). An alternate interpretation of similar data, involving unusual behavior of the probe molecule at the active site, has also been presented[64]. In all known cases of reactions involving a radical intermediate, this norcarane probe produces a product derived from the 3-cyclohexenylmethyl radical, as the major rearrangement product. The rate constant for the radical rearrangement of the 2-norcaranyl radical has been found to be $2 \times 10^8\ s^{-1}$. By contrast, for reactions proceeding through discrete carbocations, rearrangement leads instead to 3-cycloheptenol as the *major rearrangement product.*

The extent of observed rearrangement with a panel of P450 enzymes leads to a radical lifetime in the picosecond to nanosecond regime, certainly long enough to be considered an intermediate (Figure 1.5). A consistent timing was found for several similar probes that were all small, aliphatic hydrocarbons. Smaller amounts of cation-derived products were also observed and were attributed

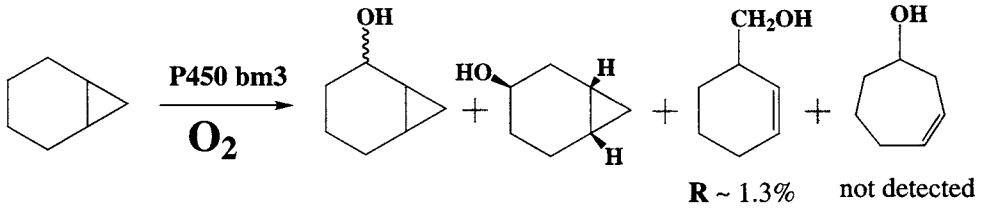

Figure 1.4. Norcarane as a molecular probe of radical intermediates during C–H hydroxylation by cytochrome P450 BM3.

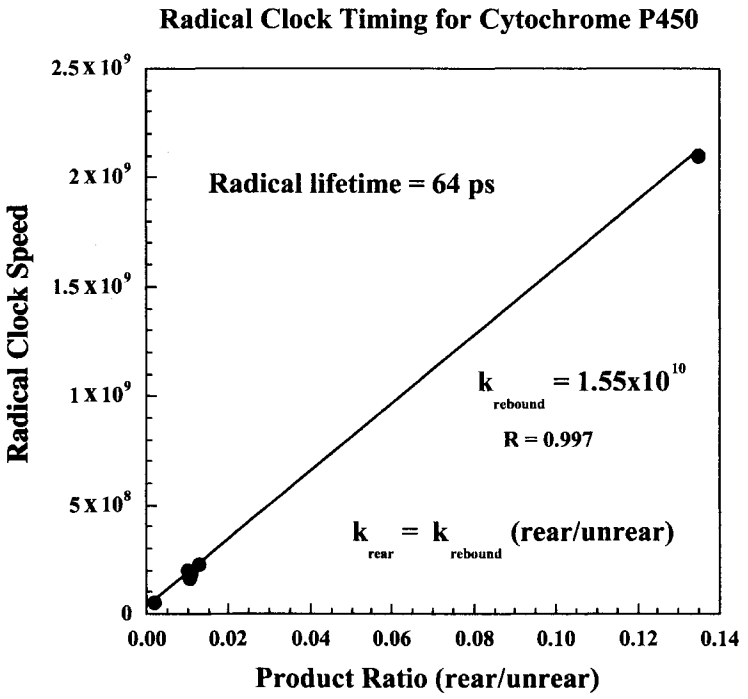

Figure 1.5. Plot of radical rearrangement rate constant vs observed product ratios for P450-mediated hydroxylation of bicyclo[2.1.0]pentane, norcarane, and spiro[2,5]octane.

to a competing electron-transfer oxidation of the incipient radical, a well-precedented process. By contrast, the hydroxylation of norcarane with a ruthenium porphyrin catalyst that proceeds through a reactive oxoruthenium(V) porphyrin intermediate, afforded *no detectable rearrangement.*

DFT calculations on the ruthenium-mediated hydroxylation show that the low-spin reaction trajectory is preferred throughout, in accord with general expectations for the behavior of second-row transition metals[65, 66]. The ruthenium analog was found to be more electrophilic than its iron complex, having lower hydrogen abstraction barriers. Thus, the data for the iron and ruthenium porphyrin systems is in accord with the predictions of theory that a radical rebound process is viable for iron which has an accessible high-spin state but not for ruthenium which is always low-spin.

The hydroxylation of camphor by an oxoferryl porphyrin has also been described by Kamachi and Yoshizawa[67]. While two spin states of the reactive intermediate were also found in this work, it was the high-spin quartet state of the oxoferryl that was lower in energy. Also significant in these calculations, were the findings that there was an interaction between the incipient substrate radical upon hydrogen abstraction and the Fe–OH center at the P450 active site and that there was a 3.3 kcal mol^{-1} activation energy for the highly exothermic radical rebound to form the product alcohol (Figure 1.6(a)). Such an interaction would be expected to *retard* radical rearrangement rates, providing another possible avenue for the mis-timing of the clocks. The reaction profile for the oxygen rebound pathway of cytochrome P450 computed by Shaik is presented in Figure 1.6(b) for comparison. Computations on the details of C–H bond cleavage in camphor by a P450 model described by Friesner have revealed an unusually low energy barrier for this process[68]. The primary contribution to stabilization of the transition state

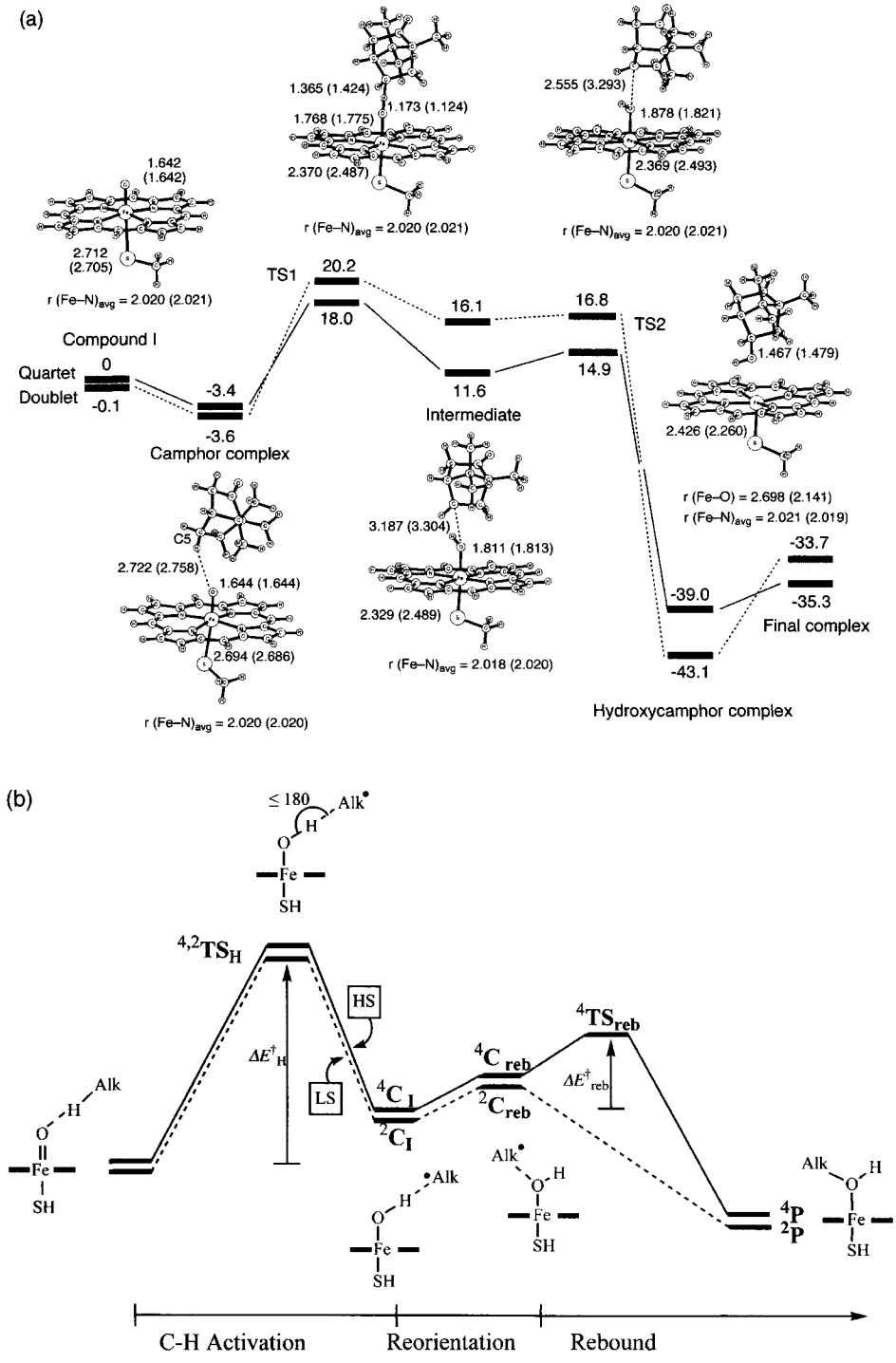

Figure 1.6. (a) Energy level diagram and reaction coordinate computed by Yoshizawa *et al.* for the hydroxylation of camphor by a ferryl–porphyrin cation radical (7). Adapted from ref. [67]. (b) Reaction profile for oxygen rebound computed by Shaik *et al.* Adapted from refs [60], [62] and unpublished material from S. Shaik.

was attributed to the interaction of positively charged residues in the active-site cavity with carboxylate groups on the heme periphery. Additional experiments on oxoferryl species of known electronic configuration would seem to be necessary to address these questions.

Other, more exotic factors such as nonstochastic behavior[69] and tunneling effects[70], could also be involved in causing the mistiming of events during C–H bond hydroxylation. Indeed, a carbene ring-expansion reaction was very recently found to have a large quantum-tunneling effect that significantly affected the observed rate[71]. High-level calculations indicated that a thermal, over-the-barrier process, and quantum tunneling of *carbon* were still competitive even at room temperature. Applied to C–H hydroxylation by a reactive oxidant, this situation could give the appearance of multiple oxidants and non-Arrhenius behavior. Further, computations have suggested that the speed of radical clocks can be made to run fast via interactions with even simple metal ion centers such as Li^+ (ref. [72]). Thus, for a stepwise reaction via the caged radical intermediate in Scheme 1.5, a spectrum of apparent lifetimes, perhaps dependent on such effects as weak dipolar interactions and even vibrational state, might be observed for rebound through transition state **R** to intermediate **8**. Consideration of the energy landscape for C–H hydroxylation (Figure 1.7) suggests that the C–H bond cleavage and concomitant FeO–H bond formation will occur *on a high-energy plateau*, since the scissile C–H bond should be similar in energy to the forming FeO–H bond. Accordingly, the intrinsic exothermicity of the hydroxylation reaction will be expressed in the C–OH bond-forming step. In such a scenario, it becomes more clear as to how small changes in bond energies and weak interactions of the reaction ensemble along the reaction coordinate could have a significant effect on the outcome, for example, positional or stereochemical scrambling, by shifting the position of the transition states along the reaction coordinates.

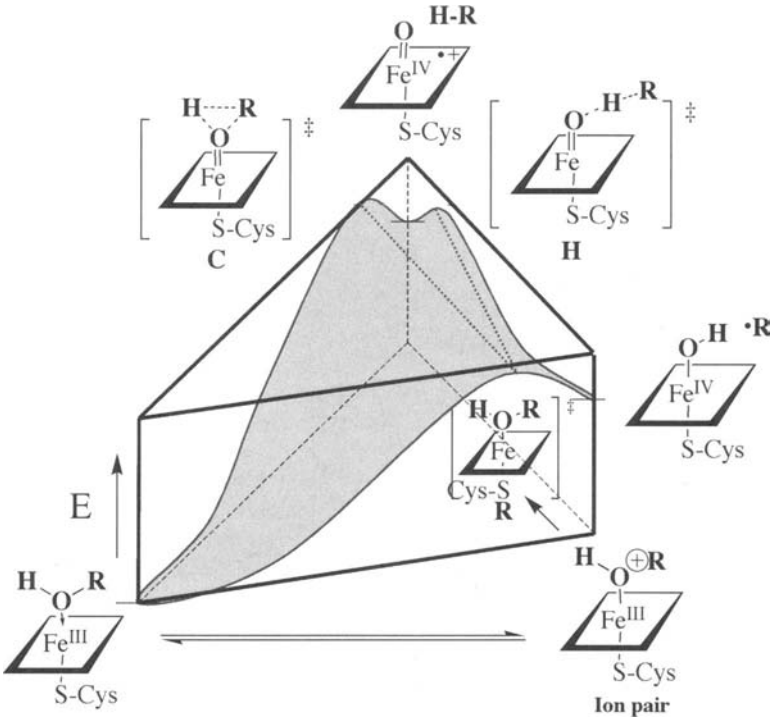

Figure 1.7. Energy landscape for aliphatic hydroxylation by cytochrome P450.

The nonheme diiron hydroxylases, such as methane monooxygenase (MMO)[73] and AlkB, the ω-hydroxylase from *P. putida*, have also yielded to similar structural, spectroscopic, and mechanistic probes. Interestingly, there are striking similarities between the consensus mechanism for the heme and nonheme iron proteins (Figure 1.8). For MMO, the resting enzyme has both iron centers in the ferric state. Reduction and binding of oxygen again produces a peroxo intermediate which is oxidized to a reactive species, compound Q, that has been characterized as a bis-μ-oxoiron(IV) intermediate. Both AlkB[74] and MMO[64, 75] have been interrogated recently with the diagnostic probe norcarane and both have shown the radical rearrangement product, hydroxymethylcyclohexene. With MMO, it was possible to show that it was the reactive intermediate Q that was interacting with the substrate probe. For the histidine-rich hydroxylase, AlkB, the results were particularly striking since 15% of the product was indicative of the radical rearrangement pathway. Similar

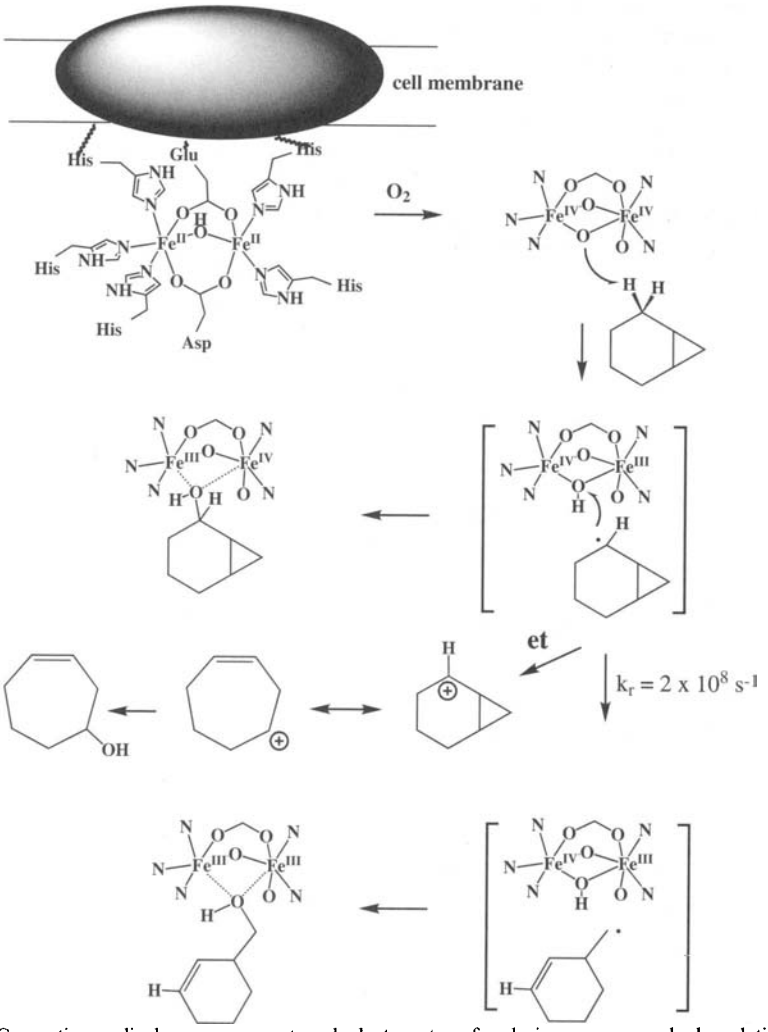

Figure 1.8. Competing radical rearrangement and electron transfer during norcarane hydroxylation by the histidine-rich hydroxylase XylM.

results have been obtained recently for the related histidine-rich, diiron hydroxylase XylM[76]. A significant aspect of this work was that it was performed on whole cells and clones into which the AlkB and XylM genes had been introduced. Thus, mechanistically informative biochemistry can be obtained from this type of biological screen.

5. On the Mechanism of Nitric Oxide Synthase

Nitric oxide (NO) is produced by the heme-containing metalloenzyme NOS (EC 1.14.13.39). Several NOS isoforms are homodimers with each monomer containing binding sites for NADPH, FMN, FAD, calmodulin, tetrahydrobiopterin (H4B), and a heme group[6]. Similar proteins are found in animals, plants, and bacteria indicating that this is a widely distributed and highly conserved process in nature. The H4B cofactor is especially important, serving structural, allosteric, and redox functions[77–80]. The X-ray crystal structures of substrate-bound NOS show that both the substrate and H4B are bound at the heme site with a substantial network of hydrogen bonds[11–13]. NOS catalyzes the two-step, five-electron oxidation of L-arginine via *N*-hydroxyarginine (NHA) to citrulline and NO (Scheme 1.6). The initial *N*-hydroxylation of L-Arg to NHA by O_2 is similar to the *C*-hydroxylations of P450 described above. The second step of the NOS reaction is unusual because it is a three-electron, aerobic oxidation of NHA to NO and citrulline[81, 82].

Our current understanding of these processes is constrained by the fact that the consensus mechanism (Scheme 1.6) contains several unknown intermediates and unprecedented processes in the second step. There have been a number of significant recent advances in the mechanistic enzymology of NOS and the structures of the enzyme–substrate complexes. However, while these results have provided confirmation of the basic tenets for the *N*-hydroxylation of arginine in the first part of the consensus mechanism, the results raise important questions regarding the oxidation of NHA and the release of NO. Thus, Poulos has shown that the X-ray structure of NOS with NO bound to the heme iron center as a structural surrogate for O_2, places the NO oxygen within hydrogen-bonding distance to the ω-N–H[13]. This juxtaposition provides support for the notion that the arginine proton assists the heterolysis of the FeO–O bond during oxygen activation to afford the ferryl intermediate in a P450-like process. However, the same structure would have

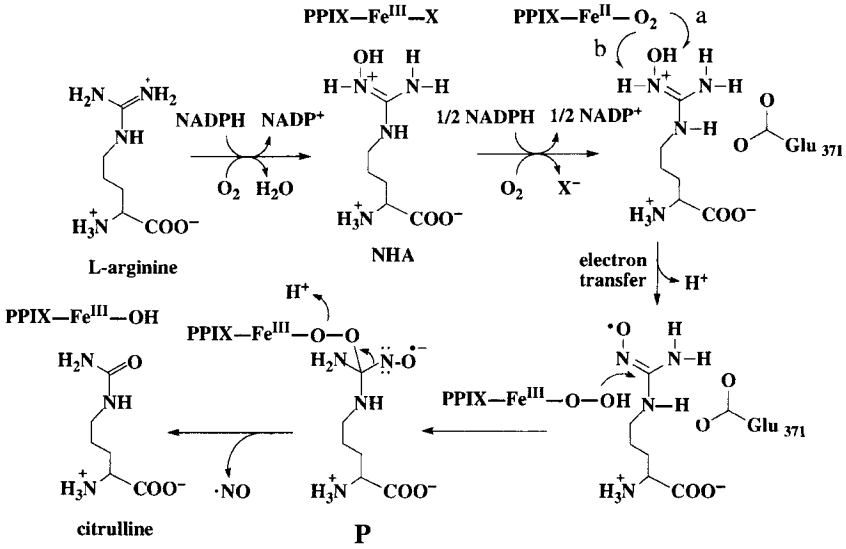

Scheme 1.6.

difficulty accommodating both the hydroxyl group of NHA where it would have to be, and the O_2 of the next cycle. Significantly, very recent EPR/ENDOR results by Hoffman *et al.*[83] have indicated that the incipient hydroxyl of NHA is formed *bound to the heme iron* in a manner similar to C–H hydroxylation by P450. This unsuspected arrangement is consistent with an oxygen rebound scenario but inconsistent with the X-ray structure of NHA bound to the active site of NOS obtained by Tainer *et al.*[11], which shows the *N*-hydroxy group to be displayed away from the heme iron. Thus, it appears that NHA, as biosynthesized from arginine, may be formed in *a non-equilibrium configuration* with respect to the NOS heme active site. In this light, the observation by Silverman[84] that oxime ethers of the type NHA–OR are active substrates for NOS and that NO is produced from these species is very informative. The NHA–NOS crystal structure suggests that NHA–OR derivatives can be accommodated at the active site in the configuration shown in Figure 1.9[85]. Thus, the O–H of NHA may not be mechanistically significant because the mechanism of the *N*-hydroxylation of L-Arg to afford NHA is still available to the oxime ethers.

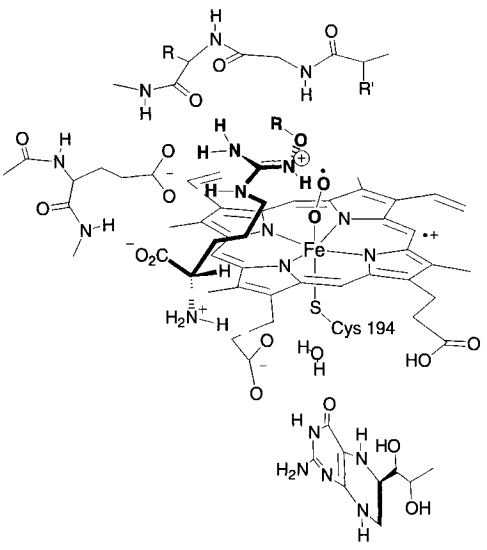

Figure 1.9. Structure suggested for the active site of RO-NHA-bound murine iNOS.

6. Synthetic Oxometalloporphyrins as Models for Cytochrome P450

Studies using synthetic metalloporphyrins (Figure 1.10) as models for cytochrome P450 have afforded important insights into the nature of the enzymatic processes[86, 87]. Indeed, each of the intermediates shown in Scheme 1.1 has been independently identified by model studies using synthetic analogs, especially *meso*-tetraaryl porphyrins[86, 88].

The first report of a simple iron porphyrin system that effected stereospecific olefin epoxidation and alkane hydroxylation was reported in 1979 (Scheme 1.7). This system introduced the use of iodosylbenzene as an oxygen-transfer agent to mimic the chemistry of cytochrome P450[89].

It was later discovered that the reactive intermediates in the iron porphyrin model systems were high-valent oxoiron porphyrin complexes. A green oxoiron(IV) porphyrin cation radical species (**13**) has been well characterized by various spectroscopic techniques, including visible spectroscopy, NMR, EPR, Mössbauer, and EXAFS (Figure 1.11)[90–98]. It has recently been shown by Nam and Que that the oxygen-atom transfer from certain iodosylarenes is reversible with some iron porphyrins. For the case of 1,2-difluoro-4-iodobenzene both an oxoferryl species and an iodosyl–ferric species were observed to be in equilibrium[99].

A family of oxoiron(IV) porphyrin cation radical species (**13**) with different axial ligands has been reported, each of which displayed a characteristic ^{1}H–NMR for the pyrrole protons. Addition of methanol replaced each of these ligands with a solvent molecule ($\delta = -22.8$)[100]. A report of the imidazole and *p*-nitrophenolate complexes of **13** has also appeared, affording closer model complexes for the compounds I of peroxidase and catalase, respectively[101]. The oxoiron(IV) porphyrin cation radical complexes **13** were shown to be highly reactive as oxygen-atom transfer agents toward olefins and hydrocarbons, that is, reacting with olefins to afford epoxides and with alkanes to give alcohols[102–104]. Notably, **13**-4-Me-Im was also reactive toward norbornene, giving a 67% yield of the corresponding epoxide[100]. Significant variations have been observed in the reactivity and

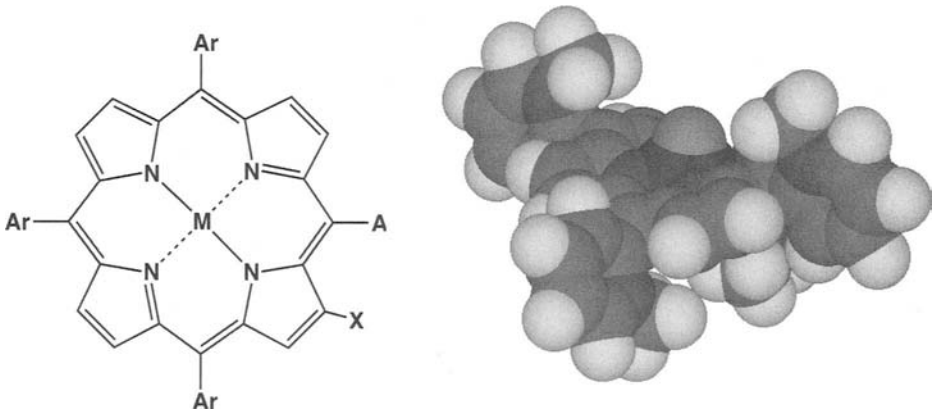

Figure 1.10. Typical synthetic tetraaryl porphyrins.

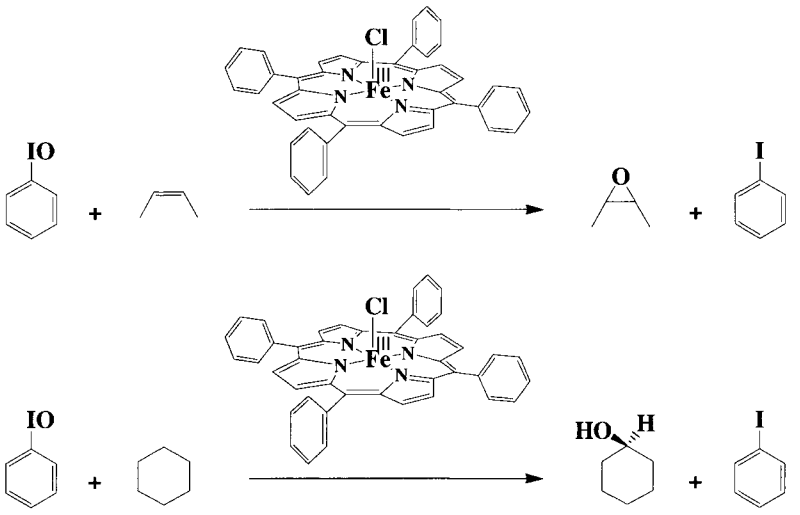

Scheme 1.7. Olefin epoxidation and alkane hydroxylation catalyzed by an iron porphyrin, $Fe^{III}(TPP)Cl$.

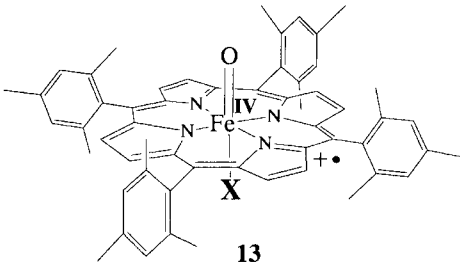

13

X = Cl δ = -9.01
O-Bz δ = -15.6
OMe δ = -16.2
4-Me-Im δ = -13.7

Figure 1.11. The family of oxoiron(IV) porphyrin cation radical species, $Fe(IV)(O)(TMP)^{+\bullet}(X)$ and the characteristic proton NMR resonances of the pyrrole protons.

selectivity of the complex **13** as a function of the axial ligand[105–107]. By contrast, the reactivity and stereospecificity of the corresponding oxoiron(IV) porphyrin complexes were low[86, 108, 109].

Nam has described studies using observed changes in product ratios and ^{18}O-labeling to suggest that *both* oxoferryl complexes such as **13** and the Fe(III)–O–X precursors are reactive oxidants[48, 110]. The nature of the anionic ligand was shown to affect both product selectivities and the efficiency of ^{18}O exchange. It is difficult, however, to discern the cause of the changes observed, since the two-oxidant scenario proposed by Nam and the anionic ligand effect on the reactivity of the oxoferryl complex itself described by Gross, both would seem to explain the results. The two most-well-characterized intermediates, $Fe(IV)(O)(por)^{+\bullet}(X)$, ("compound I") and (por)Fe(IV)=O ("compound II") are known to react with olefins to afford epoxides with different stereoselectivities. The former is known to produce a high *cis/trans* ratio of epoxide from *cis* olefins, while the latter gives mostly *trans* epoxide via a stepwise process. The effect of axial ligands would then be on the *lifetime* of $[(por)Fe(IV)=O]^{+\bullet}$ (high *cis/trans* epoxide ratio), which easily decays to (por)Fe(IV)=O (low *cis/trans* epoxide ratio). Thus, while an iron(III)(por)–peroxyacid complex has been demonstrated to be reactive toward organic substrates such as olefins, as discussed above, there is no unambiguous evidence as yet from the model studies that a hydroperoxoiron(III) porphyrin species, HOO–Fe(III)(por), is a reactive, electrophilic oxidant.

7. Manganese Porphyrins in Catalytic Oxidations

Manganese porphyrins have been shown to have unusually high reactivity toward olefin epoxidation and alkane hydroxylation[111–117]. However, the physical characteristics of the putative oxomanganese(V) porphyrin species remained particularly elusive[90, 118] because of its high reactivity and transient nature. Stable oxomanganese(V) complexes are few, the only examples involving the use of tetraanionic ligands to stabilize the high-valent manganese center[119–122].

Structurally related to the porphyrins, manganese salen catalysts have shown wide applicability for the epoxidation of unfunctionalized olefins. First described by Kochi[123], this system has been particularly effective for the asymmetric epoxidation of prochiral olefins with readily available complexes such as **11**[124]. Evidence for an oxomanganese(V) salen complex[125] and an oxoiron(IV) salen complex $[O{=}Fe(IV)(salen)]^{\bullet+}$(ref. [126]) have been presented. The area has been thoroughly reviewed[127, 128]. The reader is also referred to the growing literature on high-valent metallocorroles[129–132].

The intermediacy of reactive oxomanganese(V) porphyrin complexes has long been implicated in olefin epoxidation and alkane hydroxylation because of the distinct reactivity patterns and $H_2{}^{18}O$-exchange behavior[133–139], as compared to that of the relatively stable oxomanganese(IV) porphyrin **14** intermediates which have been isolated and well characterized[118, 140]. The oxomanganese(IV) porphyrin complex transferred oxygen to olefins with little stereoselectivity, while a transient oxomanganese(V) complex underwent oxygen transfer to olefins with predominant retention of configuration (Scheme 1.8)[134, 141]. Further, the oxomanganese(IV) species exchanged the oxo ligand with water slowly while the positively charged oxomanganese(V) complex readily exchanged the oxo ligand with added ^{18}O water[134].

Oxometalloporphyrin studies in aqueous media have allowed the study of reactive intermediates and metal–oxo–aqua interchange. The small peptide–porphyrin fragment, microperoxidase 8, has afforded evidence of reactive metal–oxo intermediates upon reaction with oxidants such as hydrogen peroxide[142, 143]. Important insights into this oxo–hydroxo tautomerism were first reported by Meunier[18, 137–139, 144]. It was shown in these studies that metal–oxo species are able to transfer an oxygen atom originating from either the oxygen source or from water. Because the intermolecular exchange of metal–oxo with water is slow, an intramolecular exchange of labeled oxygen atoms occurred, which is reminiscent of a carboxylic acid. This mechanism involves a rapid, prototropic equilibrium, probably via a *trans*-dioxoMn(V) intermediate[145], that interconverts an oxo group on one face of the metalloporphyrin with an aqua or hydroxo group on the other face. This type of rearrangement was revealed by performing a catalytic oxygenation catalyzed by a manganese porphyrin in

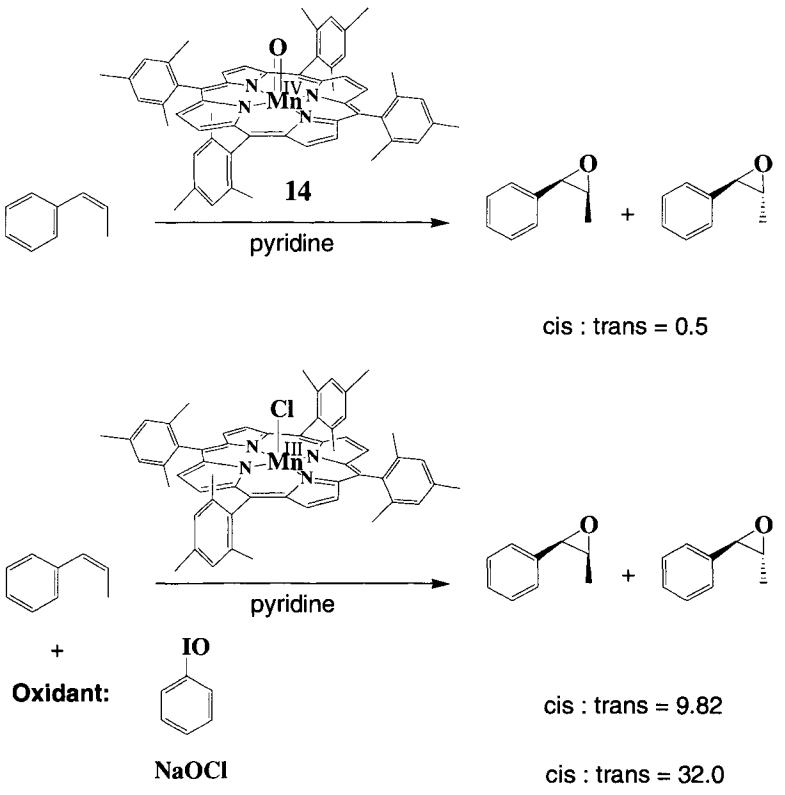

Scheme 1.8. Reactivity and stereoselectivity of oxomanganese(IV) and oxomanganese(V) (generated by Mn(III) and oxidants *in situ*) in olefin epoxidation.

^{18}O-labeled water but with a ^{16}O oxidant such a Oxone or a peroxyacid. The oxo–hydroxy tautomerism would allow as much as 50% water-derived ^{18}O oxygen transfer to a substrate, while the other 50% of the oxygen would derive from the peroxide.

$[Mn^{III}(TMPyP)]$ with a variety of oxidants, *m*-CPBA, HSO_5^-, and ClO^-, has been shown to produce the same, short-lived intermediate. An oxoMn(V) porphyrin structure was assigned to this intermediate. The rate of formation of oxoMn(V) from $Mn^{III}(TMPyP)$ followed second-order kinetics,

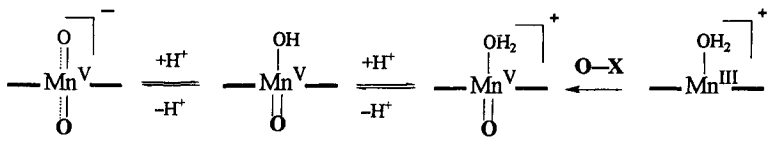

The first direct detection of an oxomanganese(V) porphyrin intermediate under ambient catalytic conditions was achieved by using rapid-mixing stopped-flow techniques[46, 146]. A direct assessment of its reactivity in both one-electron and oxygen-transfer processes was made possible by these observations. The reaction of tetra-*N*-methyl-4-pyridylporphyrinatomanganese(III) first-order in Mn(III) porphyrin, and first-order in oxidant. The rate constants have the following order: *m*-CPBA ($2.7 \times 10^7\ M^{-1}\ s^{-1}$) > HSO_5^- ($6.9 \times 10^5\ M^{-1}\ s^{-1}$) ~$ClO^-$ ($6.3 \times 10^5\ M^{-1}\ s^{-1}$). Once formed, the intermediate oxoMn(V) species was rapidly converted to oxoMn(IV) by one-electron reduction with a first-order rate constant of $5.7\ s^{-1}$. The oxoMn(IV) species was relatively

stable under the reaction conditions and was shown by EPR spectroscopy to have a high-spin quartet ground state. The one-electron reduction of oxoMn(V) to oxoMn(IV) was greatly accelerated by nitrite ion ($k = 1.5 \times 10^7\ M^{-1}\ s^{-1}$). However, the reaction between nitrite and oxoMn(IV) is much slower. The oxoMn(V) intermediate was shown to be highly reactive toward olefins, affording epoxide products. In the presence of carbamazepine, a water-soluble olefin, this oxygen transfer was extraordinarily rapid with a second-order rate constant of $6.5 \times 10^5\ M^{-1}\ s^{-1}$). By contrast, oxoMn(IV) was not capable of effecting the same reaction under these conditions. With *m*-CPBA as the oxidant in the presence of $H_2{}^{18}O$, the product epoxide was shown to contain 35% ^{18}O, consistent with an O-exchange-labile oxoMn(V) intermediate. Nitrite ion inhibited the epoxidation reaction competitively by one-electron reduction of the oxoMn(V) intermediate to the unreactive oxoMn(IV). In this way, it was possible to show that the oxo–aqua exchange rate was about $10^3\ s^{-1}$ for the *coordinated water*. Significantly, bulk water exchange was slower than oxo-transfer to the olefin under these conditions. This simple observation explains a body of often confusing data and claims in the literature in this field.

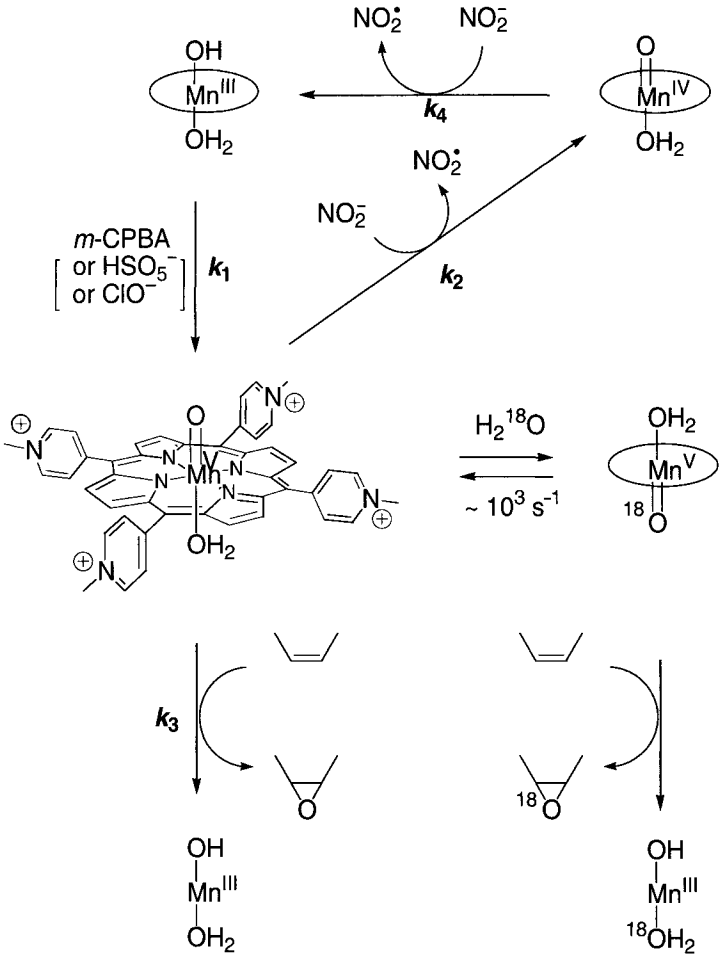

Scheme 1.9. (a) Rate constants: $k_1 = 2.7 \times 10^7\ M^{-1}\ s^{-1}$; $k_2 = 1.5 \times 10^7\ M^{-1}\ s^{-1}$; $k_3 = 6.5 \times 10^5\ M^{-1}\ s^{-1}$; $k_4 = 1.4 \times 10^2\ M^{-1}\ s^{-1}$; ^{18}O exchange $\sim 10^3\ s^{-1}$. (b) ^{18}O incorporation: 35% ^{18}O labeling from the solvent (95% $H_2{}^{18}O$) into the epoxide.

Peroxyacids will not exchange the peroxo oxygen with water at all and neither does the product epoxide. Thus, in those cases for which ^{18}O-incorporation is observed into the product epoxides or alcohols, an oxo–metal species in strongly implicated as the oxygen donor. However, failure to see ^{18}O-exchange is not a definitive result since the exchange rate may simply be too slow to compete with oxygen-atom transfer. These transformations and the ^{18}O-exchange process are summarized in Scheme 1.9. It has been shown that hydrogen peroxide is also an effective oxidant of water-soluble manganese porphyrins, affording a reactive oxoMn(V) intermediate as well[147]. With water-soluble iron porphyrins, hydrogen peroxide was able to epoxidize olefins[148]. Significantly, the efficiency of epoxidation dropped drastically above pH 5, suggesting that an acid-catalyzed heterolytic O–O bond cleavage is part of the oxygen-transfer process.

Surprisingly, the 2-*N*-methyl pyridyl isomer oxoMn(V)(TM-2-PyP) was found to be unusually stable allowing its characterization by ^1H–NMR[46]. Reaction rate constants for oxoMn(V)(TM-2-PyP) toward electron transfer, hydrogen atom abstraction, and epoxidation were all *several orders of magnitude slower* than the corresponding 4-*N*-methylpyridyl species (Scheme 1.10). This unusual effect, which did not appear in the corresponding reactions of the Mn(IV) and Mn(III) states, was ascribed to the low spin, d^2 electronic configuration of oxoMn(V). Thus, a spin-state crossover is required during reduction with the promotion of an electron from d_{xy} to $d_{xz,yz}$.

Oxomanganese(V)-5,10,15,20-tetrakis(*N*-methyl-2-pyridyl)-porphyrin (**15**) was found to transfer its oxo ligand efficiently to the bromide ion. Furthermore, this oxo transfer is *rapid and reversible*[145]. The forward reaction mimics the halide oxidation reaction catalyzed by haloperoxidases, while the reverse reaction is the catalyst activation step in substrate oxygenation by manganese porphyrins. This well-behaved equilibrium has allowed the assignment of a free energy change for this reaction and is the first clear determination of the thermodynamics of an oxo transfer reaction for a metal catalyst of this type. As can be seen in the Nernst plot in Figure 1.12, the

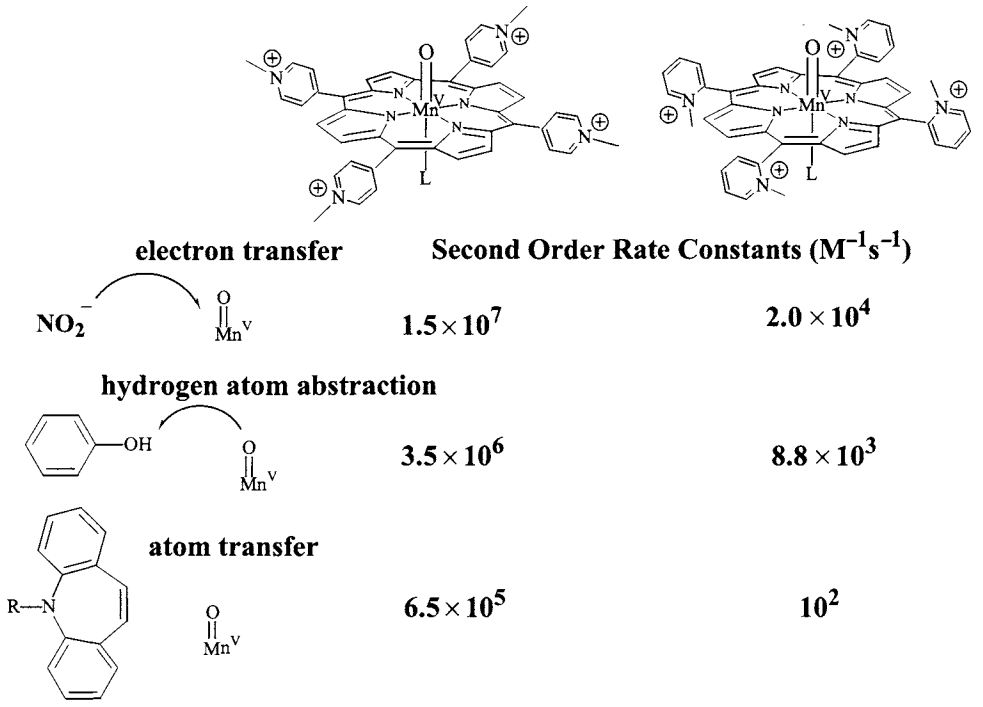

Scheme 1.10. Reaction rates for OxoMn(V)TM-4-PyP and OxoMnT(Y)M-2-PyP.

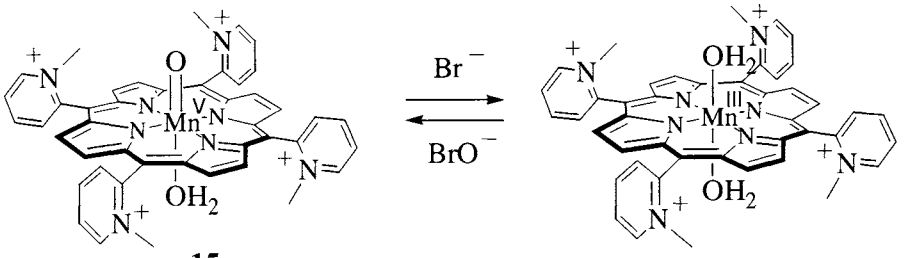

15

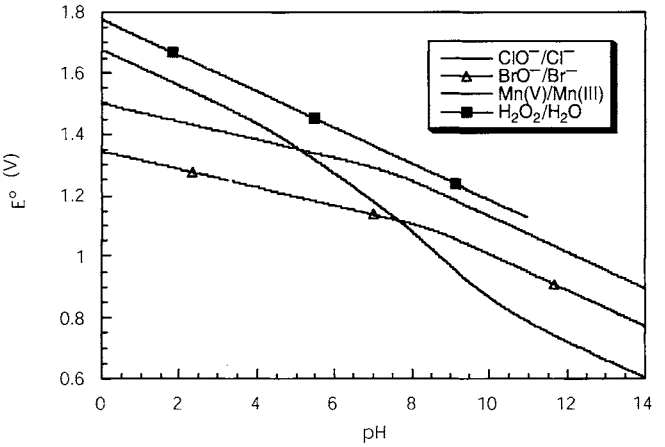

Figure 1.12. Reversible oxygen transfer from hypobromite provided an energy calibration for oxomanganese(V) porphyrins.

oxoMn(V) species is able to oxygenate bromide ion below pH 8 and chloride ion below pH 5, the increase in oxidizing power being due to the protonation of the oxoMn(V) intermediate. As can be seen, this species is tantalizingly close to the oxidation potential of water/hydrogen peroxide at low pH.

8. Metalloporphyrins as Detectors and Decomposition Catalysts of Peroxynitrite

The rapid reaction rates of peroxides with metalloporphyrins and the detection of observable oxometalloporphyrin species, especially in the reactions of manganese porphyrins with various oxidants (*m*-CPBA, NaOCl, $KHSO_5$)[146], have also inspired the use of these porphyrins as detectors for a transient biological oxidant, peroxynitrite ($ONOO^-$). $ONOO^-$, a strong one- and two-electron oxidant, has been implicated in a number of pathological conditions[149]. Structurally, $ONOO^-$ is the conjugate base of peroxynitrous acid and, like other similar peroxides, it rapidly oxidizes manganese porphyrins[136, 150, 151]. Thus, its reactions with manganese porphyrins to generate oxomanganese intermediates allowed the sensitive detection of this transient molecule under cell-like conditions[136, 150]. Using manganese porphyrins as $ONOO^-$ detectors, it has been shown that $ONOO^-$ can quickly diffuse across biological membranes and react with its biological targets[150, 152].

The fast oxidation of manganese(III) porphyrins to oxomanganese(IV) species by $ONOO^-$ satisfied the prerequisite for the porphyrins to be efficient $ONOO^-$ decomposition catalysts[150]. Indeed, manganese porphyrins, redox-coupled with biological antioxidants (such as ascorbate,

glutathione, Trolox®), rapidly reduce $ONOO^-$ and thus prevent the oxidation and nitration of biological substrates by this toxic oxidant[151, 153]. Amphiphilic analogs of the water-soluble metalloporphyrins have been developed that are suitable for liposomal delivery[154]. Further, these amphiphilic metalloporphyrins in sterically stabilized liposomes are highly active in decomposing $ONOO^-$ (ref. [154]), and thus are potential therapeutic agents for the treatment of $ONOO^-$-related diseases. Iron(III) porphyrins are also rapidly oxidized by $ONOO^-$, and Stern *et al.* have reported that water-soluble iron porphyrins have the ability to decompose $ONOO^-$ by isomerizing it to nitrate and these compounds, moreover, have shown significant biological responses in animals[155]. The mechanism of action of the iron porphyrins is significantly different than the manganese case. Significantly, *both* Fe(III) and oxoFe(IV) states are catalytically active toward $ONOO^-$ (Scheme 1.11)[156, 157]. Compounds of this sort have been shown to be highly potent in animal models of inflammation related pathologies such as diabetes and colitis[158].

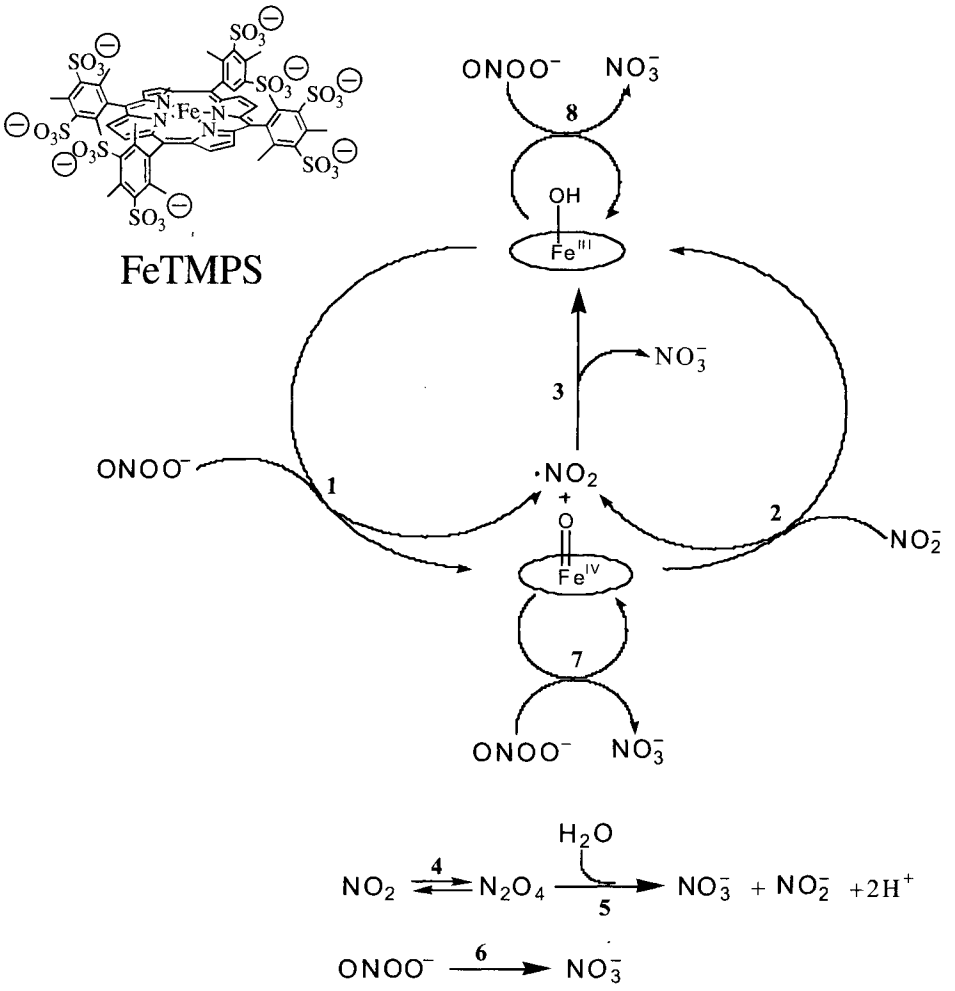

Scheme 1.11. Mechanism of peroxynitrite decomposition by FeTMPS.

9. Synthetic Metalloporphyrins as Stereoselective Catalysts

Understanding the mechanism of cytochrome P450 through the study of the synthetic model systems offers an opportunity to develop practical regioselective and stereoselective catalysts. Such catalytic systems have been extensively surveyed in numerous reviews[14, 20, 86, 159–162]. Space does not permit a discussion of all the elegant catalysts developed, but a few systems are shown here as examples.

By analogy to the natural enzymes which utilize a protein scaffold to effect substrate recognition and stereoselectivity, special steric features have been introduced into the synthetic porphyrin catalysts to achieve regio- and enantioselective oxidation. The success of such systems relies on the steric interactions between the substrates and porphyrin catalysts, which position the substrates specifically toward the reactive metal–oxo center. Breslow *et al.*[163, 164] have recently reported a remarkably selective, catalytic steroid hydroxylation using an artificial cytochrome P450 enzyme. The synthetic strategy to induce selectivity in the model system was the attachment of four cyclodextrin appendages to a synthetic manganese porphyrin used in place of the heme center of the natural enzyme. These donut shaped heptamylose sugars have a hydrophobic central cavity, which is known to bind aromatic molecules. The substrate steroid was modified with such an aromatic group at either end of the molecule. The host–guest complex obtained from these designed partners, Figure 1.13, displays a limited region of the substrate steroid in the vicinity of the catalytic manganese center. What is most significant about this artificial enzyme is the fact that hydroxylation occurred *only* at carbon 6 to give the 6α-hydroxysteroid, even though there are many sites in this molecule with similar intrinsic reactivity. This high selectivity was found to depend critically on the precise arrangement of the aromatic groups of the substrate. Moreover, the manganese porphyrin–cyclodextrin construct was able to release the product sterol and hydroxylate at least four steroid molecules. Catalytic turnover with such high positional selectivity is highly unusual for this kind of model system[167].

Collman *et al.* reported a series of "picket basket" porphyrins (Figure 1.14) which show extremely high shape selectivity (>1,000 for *cis*-2-octene vs *cis*-cyclooctene) and relatively high enantioselectivity in olefin epoxidation (*ee* around 70–85%)[159, 166]. Chiral, binaphthyl straps between adjacent *o*-aminophenyl groups have afforded very good enantiomeric selectivities for styrene epoxidations[167].

The first use of a chiral porphyrin to carry out asymmetric epoxidation was reported in 1983, giving 50% *ee* with *p*-chlorostyrene[168]. The *ee* was improved to ~70% for epoxidation of *cis*-β-methylstyrene with the use of a very robust chiral vaulted binaphthyl porphyrin **16** (Figure 1.15)[169, 170]. More significantly, this catalyst afforded the first case of catalytic asymmetric hydroxylation by a model system, giving a ~70% *ee* for hydroxylation of ethylbenzene and related hydrocarbons[169, 170].

Further developments of this system have led to studies of the binaphthyl-peptide-strapped porphyrin **17**[171]. For styrene epoxidation this chiral catalyst afforded an *ee* greater than 90% in the initial stages of the reaction, with the (*R*)-styrene oxide predominating. NMR T_1 relaxation studies with the copper(II) derivative of the same ligand

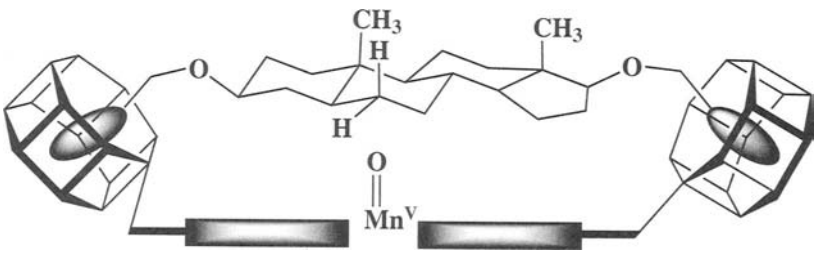

Figure 1.13. Steroid-manganese porphyrin host–guest complex.

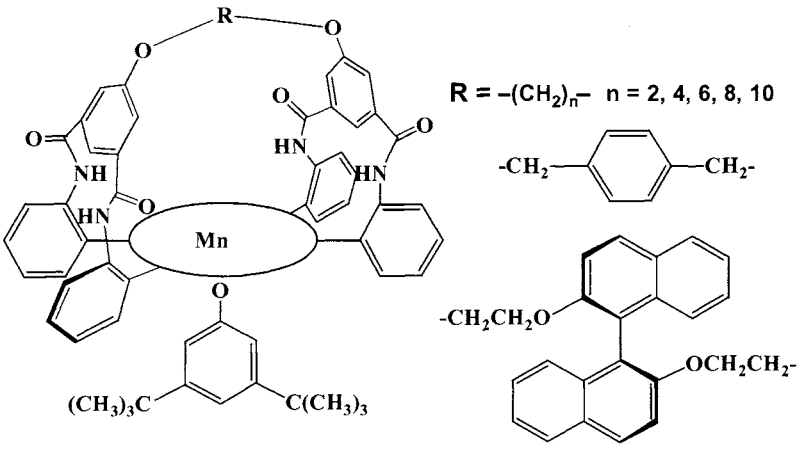

Figure 1.14. Chiral "picnic basket" porphyrins.

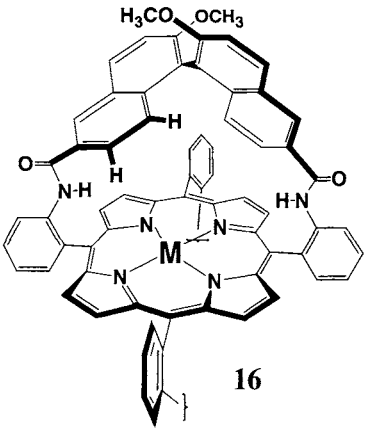

Figure 1.15. A chiral vaulted binaphthyl metalloporphyrin.

showed that it was the protons of the major enantiomer of the product epoxide that were more efficiently relaxed in an inversion-recovery experiment with **Cu-17**. Comparative T_1 data are shown in Figure 1.16. Accordingly, the major product must fit better into the chiral cavity of this catalyst. Thus, one can conclude that the enantioselectivity observed can be attributed to a simple lock-and-key process in which the transition state for epoxidation must look rather like the coordinated epoxide.

An interesting functional active-site model system for prostaglandin H synthase has recently been described by Naruta[172, 173]. In this "twin coronet" structural motif, four pendant hydroxynaphthyl groups provide a sterically encumbered, hydrophobic substrate-binding cavity (Figure 1.17). Upon treatment with *m*-chloroperoxybenzoic acid an oxoiron(IV)–naphthyloxy radical species was formed and detected by EPR. This radical intermediate reacted with a 1,4-diene and oxygen in a single-turnover reaction to afford 5-*trans*-7-*cis*-undeca-5,7-diene-4-ol in 156% yield. The formation of the aryloxy radical was shown to be essential to this conversion in close analogy to the enzymatic process.

10. Ruthenium Porphyrins in Oxidative Catalysis

The controlled oxygenation of alkanes, alkenes, and aromatic hydrocarbons is one of the most important technologies for the conversion of crude oil and natural gas to valuable commodity chemicals[174]. Biomimetic studies of metalloporphyrins have led to important advances in practical catalysis, especially with ruthenium porphyrins. Reaction of *m*-CPBA, periodate, or iodosylbenzene with Ru(II)(TMP)(CO) produced Ru(VI)(TMP)$(O)_2$[175]. Remarkably, Ru(VI)(TMP)$(O)_2$ was found to catalyze the aerobic epoxidation of olefins under mild conditions[176]. Thus, for a number of olefins including cyclooctene, norbornene, *cis*-, and *trans*-β-methyl styrene 16–45 equivalents of epoxide were

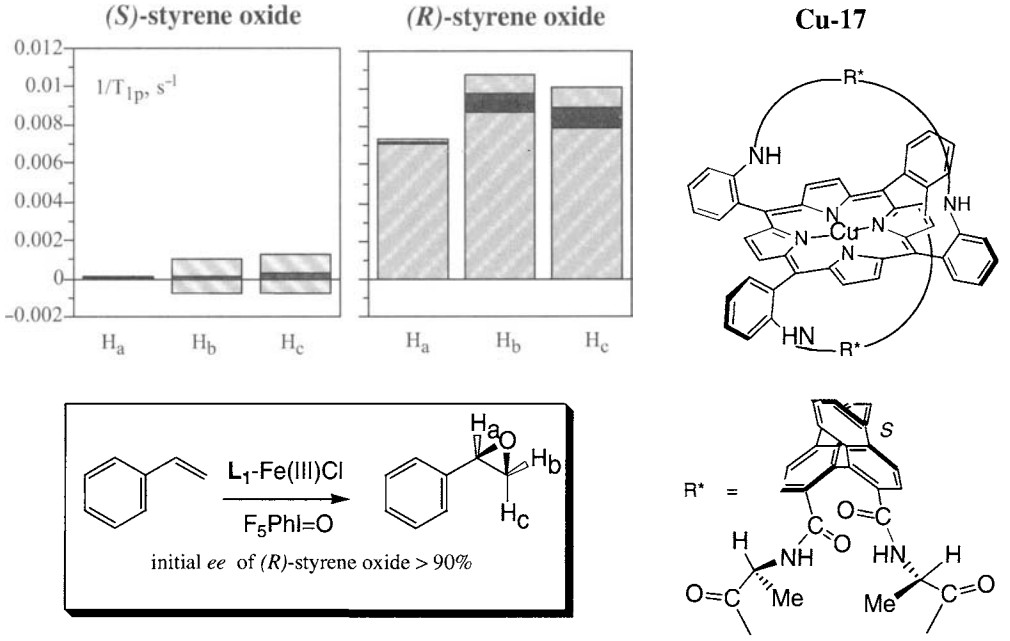

Figure 1.16. NMR T_1 relaxation data compared to stereoselectivity.

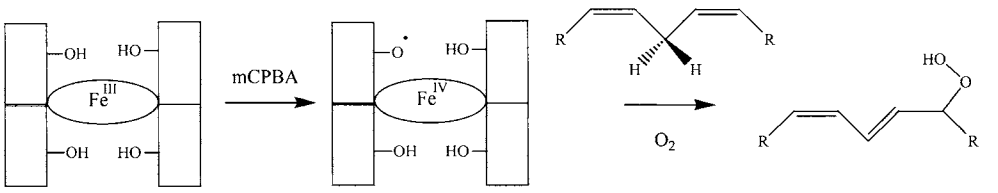

Figure 1.17. Twin coronet model prostaglandin H synthase.

produced per equivalent of the ruthenium porphyrin complex over a 24-hr period at room temperature under 1 atm of dioxygen.

Dioxygen activation by Ru(II) porphyrins is likely to involve the formation of a μ-peroxo-ruthenium(III) dimer followed by homolysis of the O–O bond to give two equivalent of oxoruthenium(IV) species. Nakamoto *et al.*[177, 178] detected such a μ-peroxoruthenium(III) intermediate by resonance Raman spectroscopy (ν_s(O=Ru) at 552 cm^{-1}) in the toluene solution of Ru(II)(TPP) saturated with O_2 at −80°C. Upon raising the temperature of the solution a ν_s(O=Ru=O) band corresponding to Ru(VI)(TMP)$(O)_2$ appeared at 811 cm^{-1}.

X-ray data obtained for a closely related Ru(VI)(TDCPP)$(O)_2$, definitively established a structural precedent for the *trans*-dioxoRu(VI) porphyrin complexes[179]. The structure revealed a nearly planar arrangement of the porphyrin macrocycle and two relatively long Ru=O bonds of 1.729 Å (Figure 1.18). Marchon and coworkers have published an X-ray structure of *trans*-dihydroxoruthenium(IV) complex of H_2TDCPP[180], also obtained from the reaction of Ru(II)(TDCPP)(CO) with *m*-CPBA. The IR spectrum of the *trans*-dihydroxoruthenium(IV) complex was reported to be different from that of the *trans*-dioxoruthenium(VI) complex. Thus, Ru(IV)(TDCPP)$(OH)_2$ showed a Ru–O stretch at 760 cm^{-1} in the IR spectrum

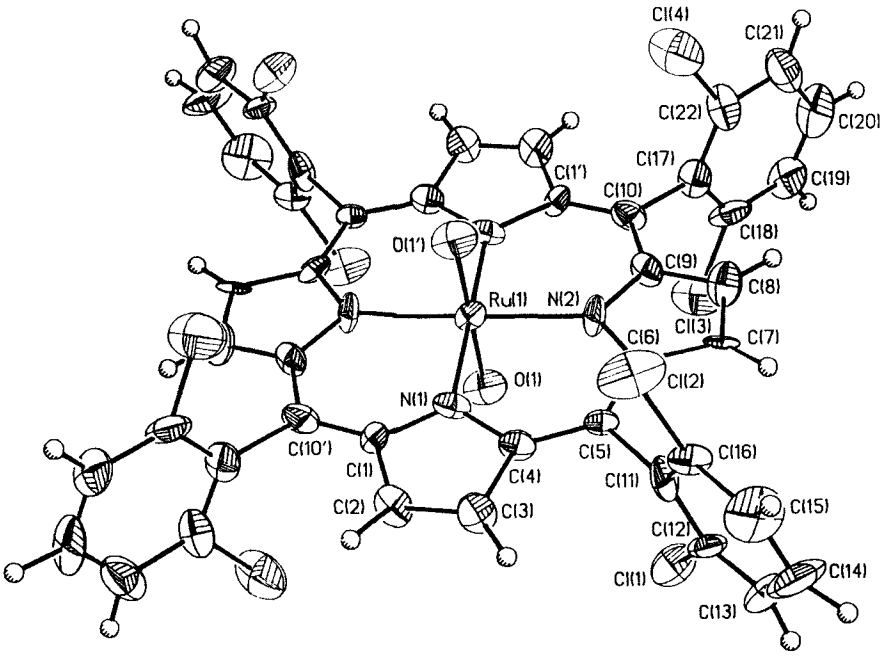

Figure 1.18. Molecular structure of $Ru(VI)(TDCPP)(O)_2$.

while the Ru=O band of $Ru(VI)(TDCPP)(O)_2$ appeared at 828 cm^{-1}. The length of the Ru–O bonds in the X-ray structure of $Ru^{IV}(TDCPP)(OH)_2$ was 1.790 Å which is somewhat longer but not significantly different from the length of the Ru=O bonds in $Ru(VI)(TDCPP)(O)_2$[179].

Nonlinear, upward U-shaped Hammett plots were obtained for the stoichiometric oxidation of substituted styrenes with $Ru(VI)(OEP)(O)_2$ and $Ru(VI)(TPP)(O)_2$. The shape of the Hammett correlations indicated a change in the structure of the transition state of epoxidation with these complexes when switching from electron-donating to electron-withdrawing substituents[181]. However, the Hammett treatment of data for a series of competitive aerobic oxidations of *para*-substituted styrenes catalyzed by $Ru(VI)(TMP)(O)_2$ gave a good linear correlation with a ρ^+ value of -0.93 against σ^+ set of parameters[179]. Only *para*-nitrostyrene deviated from the linear trend. This ρ^+ value was typical of the results obtained for iron and manganese-porphyrin-mediated epoxidations with iodosyl arenes and hypochlorite, suggesting a similar, relatively small charge separation in the transition states of these reactions[30, 166, 182, 183]. Significantly, in epoxidations with the $Ru(VI)(TPP)(O)_2/O_2$ system, the electron-rich styrenes gave more *para*-substituted phenylacetaldehyde byproducts than the electron-poor styrenes. For example, 19.5 equiv of the aldehyde and 3.8 equiv of the epoxide was produced in the oxygenation of methoxystyrene while the epoxidation of chlorostyrene produced less than 1 equiv of the aldehyde and 37 equiv of the chlorostyrene oxide based on catalyst. In order to explain these data, a mechanism has been proposed (Scheme 1.12) in which the rate-limiting-step of the initial partial charge transfer is separated from the product-forming step. Phenylacetaldehydes are believed to be formed by a 1,2-hydride shift of the cationic intermediate. This intermediate would be more favored by electron-donating *para*-substituents in agreement with the distribution of products.

Murahashi and coworkers have studied the aerobic oxidation of alkanes catalyzed by polyfluorinated metalloporphyrins including $Ru^{II}(TPFPP)(CO)$ in the presence of acetaldehyde (Scheme 1.13)[184, 185].

The catalytic oxygenation of cyclohexane and adamantane at 70°C under 1 atm dioxygen gave *c.* 200 turnovers in 24 hr. The ruthenium porphyrin

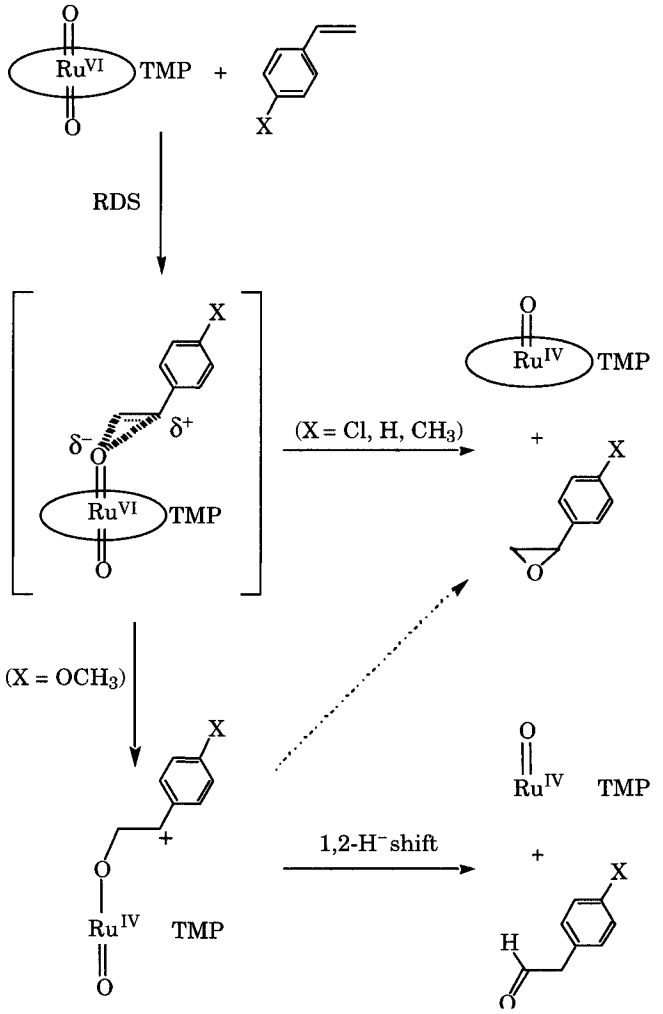

Scheme 1.12. Proposed mechanism of oxygen-atom transfer from Ru(VI)(TMP)$(O)_2$ to substituted styrenes.

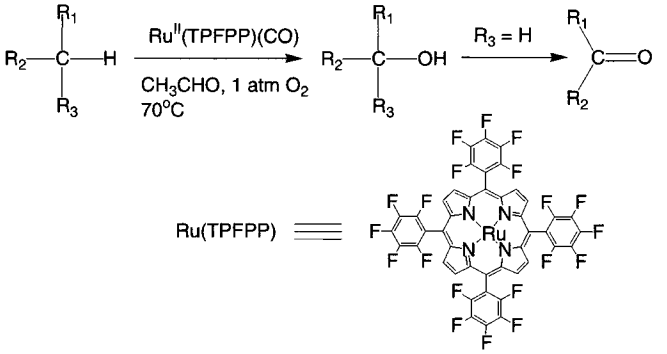

Scheme 1.13. Aerobic oxidation catalyzed by Ru(II)(TPFPP)CO, see references 184 and 185.

demonstrated high stability toward oxidative degradation with turnover numbers as high as 14,000, achieved in the oxygenation of cyclohexane when a low catalyst concentration was used. The normalized 3°/2° C–H bond preference in oxidation of adamantane with this system was about 20. Competitive experiments with cyclohexane and cyclohexane-d_{12} resulted in an isotope effect of 13. The mechanism of catalysis was not clear. It is known that the reaction of aldehydes with dioxygen in the presence of metal complexes produces peroxyacids[186]. The authors suggested an oxometal species which is formed by reaction of peroxyacid with ruthenium porphyrin as the active intermediate although no good evidence in favor of such species was presented. The possibility of a radical autoxidation mechanism cannot be excluded.

Labinger and coworkers[187] have investigated the catalysis of aerobic olefin oxidation by a highly electron-deficient perhalogenated ruthenium porphyrin complex $Ru^{II}(TPFPPPCl_8)(CO)$. The oxidation of cyclohexene under 1 atm dioxygen at room temperature proceeded mostly in the allylic positions affording 58% 2-cyclohexen-1-ol and 27% 2-cyclohexen-1-one along with only 15% of cyclohexene oxide. Three hundred turnovers of oxidation were achieved in 24 hr and 90% of the catalyst was recovered at the end of the reaction. Oxygenation of styrene gave benzaldehyde (3 turnovers in 24 hr) as the only product. By contrast, the oxidation of cyclooctene produced cyclooctene oxide as the major product (42 turnovers in 24 hr). With iodosylbenzene as oxidant $Ru^{II}(TPFPPPCl_8)(CO)$ demonstrated significantly higher selectivity for epoxidation with 81% styrene oxide and 42% cyclohexene oxide produced, based on the total amounts of oxidation products. The *trans*-dioxoruthenium(VI) complex $Ru^{VI}(TPFPPPCl_8)(O)_2$ prepared by oxidation of $Ru^{II}(TPFPPPCl_8)(CO)$ with *m*-CPBA was found to be a less efficient catalyst for the aerobic oxygenations and therefore an unlikely intermediate in the catalytic cycle. The authors noted that the distribution of products in a cyclohexene oxygenation with $Ru^{II}(TPFPPPCl_8)(CO)$ was identical to the ratio of allylic oxidation vs epoxidation products obtained in the aerobic oxidation with $Fe^{III}(TPFPPBr_8)Cl$[188]. For the iron porphyrin catalyst these reactions have been established to follow a radical autoxidation mechanism[188, 189].

Nitrous oxide is produced as a byproduct in multimillion lb/year quantities in nylon manufacture worldwide. Currently, there is a great interest toward the utilization of N_2O due to the environmentally hazardous nature of this gas with respect to the greenhouse effect and ozone layer depletion. In addition to their ability to utilize dioxygen for catalytic hydrocarbon oxidations, ruthenium porphyrins have been shown to activate nitrous oxide[190] which is an extremely inert molecule[191] and a poor ligand.[192a] Groves and Roman have found that N_2O reacted with $Ru^{II}(TMP)(THF)_2$ in toluene to produce $Ru^{VI}(TMP)(O)_2$[190]. The *trans*-dioxoRu(VI) complex can in turn epoxidize a suitable substrate such as *trans*-β-methyl styrene. This system was subsequently shown to be catalytic under appropriate conditions[192b].

Hirobe and coworkers were the first to use an unusual class of oxidants, 2,6-disubstituted pyridine *N*-oxides, in conjunction with ruthenium porphyrins for oxidation of olefins (Scheme 1.14), alcohols, and sulfides[193–197].

The epoxidation of styrene with 2,6-dichloropyridine *N*-oxide was efficiently catalyzed by of $Ru(VI)(TMP)(O)_2$ or Ru(II)(TMP)(CO) to afford styrene oxide with high selectivity and nearly quantitative yields based on substrate used[196]. Moderate yields of the epoxide (26%) were obtained with Ru(II)(TPP)(CO). Turnover numbers up to 16,500 were achieved in epoxidation of norbornene in the presence of catalytic amounts of $Ru(VI)(TMP)(O)_2$. The catalytic reactions were

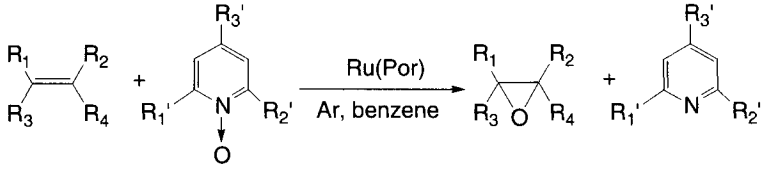

Scheme 1.14. RuPor = Ru(II)(TMP)(CO), Ru(II)(TPP)(CO) or $Ru(VI)(TMP)(O)_2$.

characterized by high chemoselectivity and stereospecificity. For example, when a 1:1 mixture of *cis*- and *trans*-stilbene was reacted with 2,6-lutidine *N*-oxide in the presence of Ru(VI)(TMP)$(O)_2$, *cis*-stilbene oxide was produced in 87% yield, while only 1% of *trans*-stilbene was epoxidized[198]. Further, the *cis* disubstituted double bond of *trans,cis,trans*-1,5,9-cyclododecatriene was predominantly oxidized under these conditions. *Cis*-stilbene was stereospecifically epoxidized with 2,4,6-trimethylpyridine. Only ruthenium porphyrins displayed catalytic activity with respect to the oxygen transfer from pyridine *N*-oxides. Other metalloporphyrins, such as Mn, Fe, Co, Mo, and Rh porphyrin complexes, were found to be inactive with these oxidants[193, 196].

While alkanes and aliphatic alcohols were inert with respect to the RuPor/*N*-oxide system, the catalytic activity of ruthenium porphyrins was dramatically enhanced in the presence of protic acids such as HBr[196, 198, 199]. Hydroxylation of adamantane with 2,6-dichloropyridine *N*-oxide in the presence of Ru(II)(TMP)(CO) and HBr afforded over 100,000 turnovers of the tertiary C–H oxidation products, 1-adamantanol and 1,3-adamantanediol, with a turnover frequency of 5.6 turnovers s^{-1}. Methylcyclohexane was selectively hydroxylated to give 1-methylcyclohexanol in 94% yield. *Cis*-9-decalol was the major product in oxidation of *cis*-decalin with no stereoisomer *trans*-9-decalol detected. Oxygenation of a relatively inactive alkane such as cyclooctanol afforded *c.* 300 turnovers of cyclooctanone (77% yield based on substrate)[196].

Nagano *et al.* have studied the oxidation of steroids with 2,6-dichloropyridine *N*-oxide catalyzed by Ru(II)(TPP)(CO), Ru(II)(TMP)(CO), and Ru(II)(TDCPP)(CO) in the presence of HBr[200]. Tertiary C–H positions of steroidal substrates were hydroxylated with complete retention of configuration of the asymmetric centers. The regioselectivity of oxidation significantly depended on the steric bulk of the *ortho* substituents of the aromatic rings at the *meso* position of the porphyrin catalysts and on the electronic properties of the porphyrins.

A very promising system for hydrocarbon oxygenation with 2,6-dichloropyridine *N*-oxide in the presence of electron-deficient, polyhalogenated ruthenium porphyrins has been reported[201, 202]. The oxidations with this system were characterized by high rates and selectivity even under mild conditions and, most significantly, could be carried out in a nonacidic reaction media. Carbonyl (5,10,15,20-tetrapentafluorophenylporphyrinato) ruthenium(II)—Ru(II)(TPFPP)(CO) showed unusually high activity with 2,6-dichloropyridine *N*-oxide as the oxygen donor (Scheme 1.15).

Adamantane and *cis*-decalin were hydroxylated with high selectivity, complete stereo-retention, extraordinarily high rates (up to 800 turnovers min^{-1}), and high efficiency with up to 15,000 turnovers. Similar conversions were obtained when Ru(VI)(TPFPP)$(O)_2$ and Ru(VI)(TPFPBr_8P)$(O)_2$ were used as catalysts. Oxygenation of less reactive substrates such as benzene and cyclohexane proceeded with lower but still significant turnover numbers (100–3,000). Tertiary vs secondary selectivity in adamantane oxidation was above 210. No rearrangement products were detected in *cis*-decalin hydroxylation.

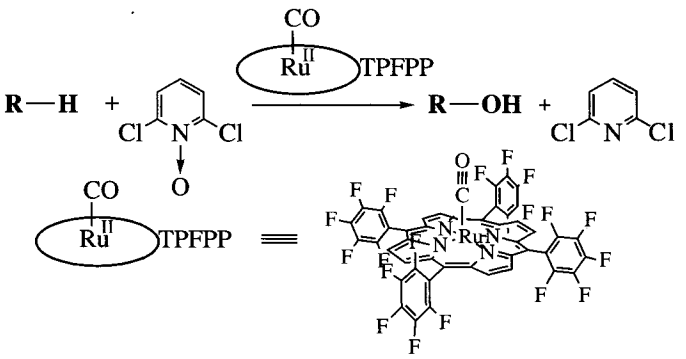

Scheme 1.15. Fast catalytic hydroxylation with a fluorophenylruthenium porphyrin.

The kinetics of product evolution in a typical reaction of adamantane hydroxylation showed an initial induction period followed by a fast, apparently zero-order phase with the maximum rate and highest efficiencies (Figure 1.19). Deviation from linear behavior took place only after 90% of the oxygen donor and 80% of the substrate had been consumed. When Ru(VI)(TPFPP)$(O)_2$, prepared by reaction of Ru(II)(TPFPP)(CO) with 3-chloroperoxybenzoic acid was used as the catalyst, no induction time was detected and zero-order kinetics were observed as well. The well-defined and characteristic UV–vis spectra of metalloporphyrins provide an invaluable tool for the mechanistic studies. Thus, monitoring the state of the metalloporphyrin catalysts during the course of both model reactions by UV–vis spectroscopy revealed that the initial form of the catalyst remained the predominant one throughout the oxidation, that is, in the Ru(II)(TPFPP)(CO)-catalyzed reaction *c.* 80% of the porphyrin catalyst existed as Ru(II)(TPFPP)(CO) and in Ru(VI)(TPFPP)$(O)_2$-catalyzed reaction more than 90% of the catalyst was still in the form of Ru(VI)(TPFPP)$(O)_2$ despite the high turnover numbers reached (~400 turnovers). The fact that Ru(II)(TPFPP)(CO) demonstrates similar and even higher maximum turnover rate of 4.9 turnovers min^{-1} in adamantane hydroxylation vs 4.0 turnovers min^{-1} for Ru(VI)(TPFPP)$(O)_2$ under the same conditions indicates that an active catalyst species *other than* Ru(VI)(TPFPP)$(O)_2$ is involved in the fast catalytic hydroxylation.

Therefore, a typical *trans*-dioxoRu(VI)–oxoRu(IV) catalytic cycle can be ruled out as the primary reaction pathway in case of rapid catalytic oxygenation. The apparent zero-order kinetics observed are consistent with a steady-state catalytic regime accessible from different initial states of ruthenium metalloporphyrin. Indeed, common oxidants, other than aromatic *N*-oxides, such as iodosylbenzene, magnesium monoperoxyphthalate, Oxone®, and tetrabutylammonium periodate produced the *trans*-dioxoRu(VI) species from Ru(II)(TPFPP)(CO) under reaction conditions but were ineffective for the rapid catalysis.

A two-electron oxidation of Ru(II)(TPFPP)(CO) would produce oxoRu(IV) porphyrin and eventually dioxoRu(VI). What is the alternative pathway for Ru^{II}(TPFPP)(CO) activation? It is known that ruthenium(II) π-cation radicals are formed from the corresponding carbonyl compounds by chemical or electrochemical one-electron oxidation[203]. Such species have been

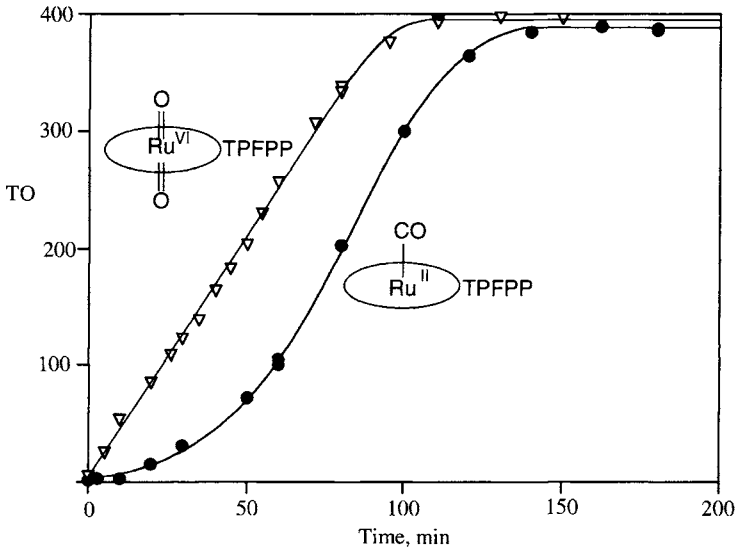

Figure 1.19. Adamantane hydroxylation catalyzed by Ru(II)(TPFPP)(CO) and Ru(VI)(TPFPP)$(O)_2$, [adamantane] = [$pyCl_2NO$] = 0.02 M, [catalyst] = 50 μM, CH_2Cl_2, 40°C. TO (Turnovers) = moles of product/moles of catalyst.

shown to undergo intramolecular electron transfer upon axial ligation and removal of CO to give ruthenium(III) porphyrins[204]. An emerald green solution of Ru(II)(TPFPP)(CO)$^{+\bullet}$ radical cation with a strong EPR signal (g = 2.00) was quantitatively obtained when Ru(II)(TPFPP)(CO) was oxidized with ferric perchlorate in methylene chloride. An EPR signal typical of a ruthenium(III) species ($g_{\|}$ = 2.55, $g_{\perp}$ = 2.05) was detected after the addition of 2,6-lutidine *N*-oxide to the solution of the radical cation.

Metastable Ru(III) and oxoRu(V) species have been proposed as key intermediates in the catalytic cycle of "rapid oxygenation" which can be viewed as a part of the general scheme of diverse oxidative chemistry of ruthenium porphyrins (Scheme 1.16). The aerobic oxygenation pathway, involving the even oxidation states, is shown in the left half of Scheme 1.16. The new fast catalytic process on the right half of the figure depicts the chemical interconnectivity between the fast and slow catalytic regimes.

Enantioselective epoxidation of unfunctionalized olefins is an important area of asymmetric synthesis[185, 205, 206]. Metalloporphyrins represent an attractive foundation for the design of the new chiral epoxidation catalysts due to their high intrinsic stability with respect to oxidative degradation. Thus, extremely large turnover numbers in the oxygenation of hydrocarbons, approaching 10^5–10^6, have been achieved with achiral metalloporphyrin catalysts[199, 207].

Gross *et al.* reported the first use of a chiral ruthenium porphyrin Ru^{II}(L_1)(CO) as a catalyst for styrene epoxidation[208]. Chiral ruthenium porphyrin systems have also been reported by Che *et al.*[209, 210]. The utilization of another chiral ruthenium porphyrin, Ru^{II}(L_2)(CO) as a catalyst for enantioselective epoxidation of olefins with 2,6-dichloropyridine *N*-oxide has been described by Berkessel and Frauenkron[211]. The highest enantiomeric excesses of the oxiranes were obtained in the epoxidation of tetrahydronaphthalene and styrene, 77% and 70% *ee*, respectively, with high yields (up to 88%). Terminal aliphatic olefins and *trans*-disubstituted olefins, represented by 1-octene and *trans*-stilbene, were sluggish substrates and gave low *ee*'s. The epoxidation of tetrahydronaphthalene with iodosylbenzene catalyzed by Ru(II)(L_2)(CO) produced only 52% *ee*

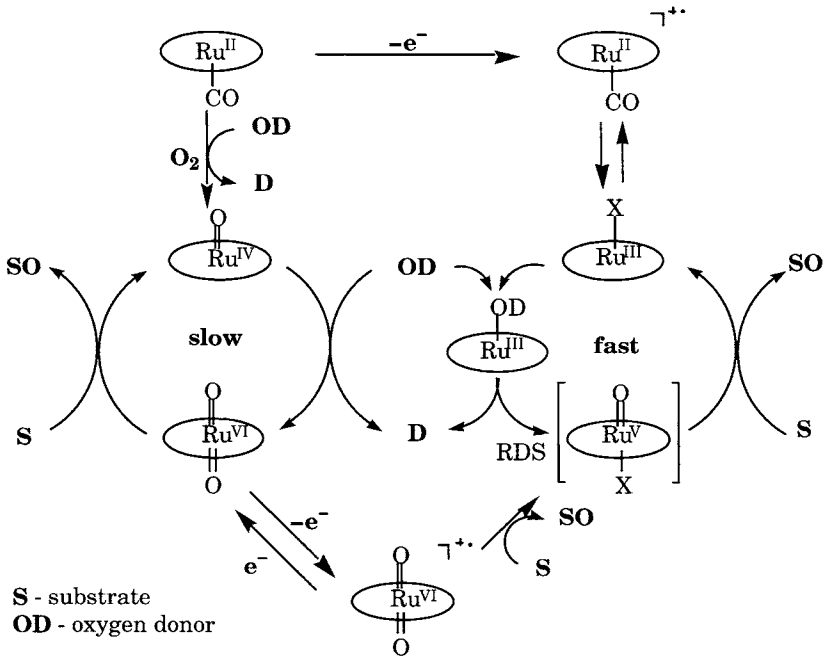

Scheme 1.16. Mechanisms of ruthenium porphyrin oxidation catalysis.

of the epoxide. Interestingly, the results were similar to those published by Gross *et al.*[107] in that the enantioselectivity of epoxidation with Ru(II)(L_2)(CO) was different when iodosylbenzene or pyridine *N*-oxides were used as primary oxidants but did not depend on the nature of the pyridine *N*-oxide. Under the comparable reaction conditions ~72% *ee* of tetrahydronaphthalene oxide was reported for the catalytic oxidation of tetrahydronaphthalene with 2,6-dichloropyridine *N*-oxide, 2,6-dibromopyridine *N*-oxide, and *N*-methylmorpholine *N*-oxide.

11. Conclusion

Cytochrome P450 has been called the Rosetta Stone of iron proteins. Perhaps nowhere else in the biological sciences has the rich interplay between structural, spectroscopic, mechanistic, computational, and chemical modeling techniques led to such a detailed level of understanding of such an important system. The central paradigm of biological oxygen activation is now recognized to involve the formation a ferryl, or oxoiron intermediate. Oxoiron(IV) porphyrin cation radicals have been observed in peroxidase, cytochrome oxidase, CPO, cytochrome P450, and in a variety of model systems. Model system studies, especially those of iron, manganese, and ruthenium porphyrins and related ligands, have led to important advances in catalysis and in catalytic asymmetric oxygenation. Advances in computational studies of such complex, open-shell systems have begun to provide a rigorous physical underpinning for the body of complex and sometimes confusing experimental results. In this chapter, I have tried to weave together all of these aspects to provide for the reader a unified picture of the current understanding in the field of cytochrome P450 research. More detailed presentations are to be found in the chapters that follow.

Acknowledgments

Special thanks are due to all the members of my research group and my collaborators who participated in the projects described here from our laboratory and contributed so many ideas, inspirations, and insights. Their names are indicated in the referenced papers. Thanks go also to the many colleagues around the world who have brought such energy and excitement to the P450 and metalloporphyrin fields for nearly three decades. Research in our laboratories was supported by the National Institutes of Health (NIGMS) and the National Science Foundation. I also thank the National Science Foundation and the Department of Energy for their support of the Environmental Molecular Science Institute (CEBIC) at Princeton University.

References

1. Hayaishi, O., M. Katagiri, and S. Rothberg (1955). Mechanism of the pyrochatecase reaction. *J. Am. Chem. Soc.* **77**, 5450–5451.
2. Tchen, T.T. and K. Block (1956). On the mechanism of cyclization of squalene. *J. Am. Chem. Soc.* **78**, 1516–1517.
3. Ortiz de Montellano, P.R. and J.J. De Voss (2002). Oxidizing species in the mechanism of cytochrome P450. *Nat. Prod. Rep.* **19**, 477–493.
4. Sundaramoorty, M., J. Terner, and T.L. Poulos (1995). The crystal structure of chloroperoxidase: A heme peroxidase-cytochrome P450 functional hybrid. *Structure* **3**, 1367–1377.
5. Manoj, K.M. and L.P. Hager (2001). Utilization of peroxide and its relevance in oxygen insertion reactions catalyzed by chloroperoxidase. *Biochim. Biophy. Acta* **1547**, 408–417.
6. (a) Groves, J.T. and C.C.-Y. Wang (2000). Nitric oxide synthase: Models and mechanisms. *Curr. Opin. Chem. Biol.* **4**, 687–695; (b) Mansuy, D. and J.L. Boucher (2002). Oxidation of N-hydroxyguanidines by cytochromes P450 and NO-synthases and formation of nitric oxide, *Drug Metab. Rev.* **34**(3), 593–606.
7. Santhanam, L. and J.S. Dordick (2002). Chloroperoxidase-catalyzed epoxidation of styrene in aqueous and nonaqueous media. *Biocatal. Biotransform.* **20**, 265–274.
8. Rantwijk, F. and R.A. Sheldon (2000). Selective oxygen transfer catalysed by peroxidases: Synthetic and mechanistic aspects. *Curr. Opin. Biotech.* **11**, 554–564.
9. Van Beilen, J.B. and Z. Li (2002). Enzyme technology: An overview. *Curr. Opin. Biotech.* **13**, 338–344.
10. Glieder, A., E.T. Farinas, and F.H. Arnold (2002). Laboratory evolution of a soluble, self-sufficient, highly active alkane hydroxylase. *Nat. Biotechnol.* **20**, 1135–1139.

11. Crane, B.R., A.S. Arvai, S. Ghosh, E.D. Getzoff, D.J. Stuehr, and J.A. Tainer (2000). Structures of the N-omega-hydroxy-L-arginine complex of inducible nitric oxide synthase oxygenase dimer with active and inactive pterins. *Biochem.* **39**, 4608–4621.
12. Raman, C.S., H.Y. Li, P. Martasek, G. Southan, B.S.S. Masters, and T.L. Poulos (2001). Crystal structure of nitric oxide synthase bound to nitro imdazole reveals a novel inactivation mechanism. *Biochemistry* **40**, 13448–13455.
13. Li, H.Y., C.S. Raman, P. Martasek, B.S.S. Masters, and T.L. Poulos (2001). Crystallographic studies on endothelial nitric oxide synthase complexed with nitric oxide and mechanism-based inhibitors. *Biochemistry* **40**, 5399–5406.
14. Fujii, H. (2002). Electronic structure and reactivity of high-valent oxo iron porphyrins. *Coord. Chem. Rev.* **226**, 51–60.
15. Woggon, W.-D., H.-A. Wagenknecht, and C. Claude (2001). Synthetic active site analogues of heme-thiolate proteins characterization and identification of intermediates of the catalytic cycles of cytochrome P450cam and chloroperoxidase. *J. Inorg. Biochem.* **83**, 289–300.
16. Ortiz de Montellano, P.R. (ed.) (1995). *Cytochrome P-450: Structure, Mechanism and Biochemistry*, 2 edn. Plenum Press, New York.
17. Guengerich, F.P. (2001). Common and uncommon cytochrome P450 reactions related to metabolism and chemical toxicity. *Chem. Res. Toxicol.* **14**, 611–650.
18. Meunier, B. and J. Bernadou (2002). Metal-oxo species in P450 enzymes and biomimetic models. Oxo-hydroxo tautomerism with water-soluble metalloporphyrins. *Top. Catal.* **21**, 47–54.
19. Groves, J.T. (2003). The bioinorganic chemistry of iron in oxygenases and supramolecular assemblies. *Proc. Nat. Acad. Sci. USA* **100**, 3569–3574.
20. Shteinman, A.A. (2001). The role of metal-oxygen intermediates in biological and chemical monooxygenation of alkanes. *Russ. Chem. Bull.* **50**, 1795–1810.
21. Makris, T.M., R. Davydov, I.G. Denisov, B.M. Hoffman, and S.G. Sligar (2002). Mechanistic enzymology of oxygen activation by the cytochromes P450. *Drug Metab. Rev.* **34**, 691–708.
22. Watanabe, Y. and H. Fujii (2000). Characterization of high-valent oxo-metalloporphyrins. In B. Meunier (ed.), *Structure and Bonding*, Vol 97, Springer-Verlag, Berlin, pp. 61–89.
23. McLain, J., J. Lee, and J.T. Groves (1999). Biomimetic oxygenations related to cytochrome P450: Metal-oxo and metal-peroxo intermediates. In B. Meunier (ed.), *Biomimetic Oxidations*. ICP Publishers, pp. 91–170.
24. Groves, J.T., R.C. Haushalter, M. Nakamura, T.E. Nemo, and B.J. Evans (1981). High-valent iron-porphyrin complexes related to peroxidase and cytochrome P-450. *J. Am. Chem. Soc.* **102**, 2884–2886.
25. Groves, J.T. and G.A. McClusky (1976). Aliphatic hydroxylation via oxygen rebound. Oxygen transfer catalyzed by iron. *J. Am. Chem. Soc.* **98**, 859.
26. Schunemann, V., C. Jung, J. Terner, A.X. Trautwein, and R. Weiss (2002). Spectroscopic studies of peroxyacetic acid reaction intermediates of cytochrome P450cam and chloroperoxidase. *J. Inorg. Biochem.* **91**, 586–596.
27. Kellner, D.G., S.C. Hung, K.E. Weiss, and S.G. Sligar (2002). Kinetic characterization of compound I formation in the thermostable cytochrome P450 Cyp119. *J. Biol. Chem.* **277**, 9641–9644.
28. Gelb, M.H., D.C. Heimbrook, P. Malkonen, and S.G. Sligar (1982). Stereochemistry and deuterium isotope effects in camphor hydroxylation by the cytochrome P450cam monoxygenase system. *Biochemistry* **21**, 370–377.
29. Groves, J.T. and D.V. Adhyam (1984). Hydroxylation by cytochrome P-450 and metalloporphyrin models. Evidence for allylic rearrangement. *J. Am. Chem. Soc.* **106**, 2177–2181.
30. Traylor, T.G. and F. Xu (1988). Model reactions related to cytochrome P-450. Effects of alkene structure on the rates of epoxide formation. *J. Am. Chem. Soc.* **110**, 1953–1958.
31. Fish, K.M., G.E. Avaria, and J.T. Groves (1988). Rearrangement of alkyl hydroperoxides mediated by cytochrome P-450: Evidence for the oxygen rebound mechanism, In J. Miners, D.J. Birkett, R. Dew, B.K. May and M.E. McManus (eds.), *Microsomes and Drug Oxidations*. Taylor and Francis, New York, pp. 176–183.
32. Kupfer, R., S.Y. Liu, A.J. Allentoff, and J.A. Thompson (2001). Comparisons of hydroperoxide isomerase and monooxygenase activities of cytochrome P450 for conversions of allylic hydroperoxides and alcohols to epoxyalcohols and diols: Probing substrate reorientation in the active site. *Biochemistry* **40**, 11490–11501.
33. Vaz, A.D.N., D.F. McGinnity, and M.J. Coon (1998). Epoxidation of olefins by cytochrome P-450: Evidence from site-specific mutagenesis for hydroperoxo-iron as an electrophilic oxidant. *Proc. Natl. Acad. Sci. USA*, **95**, 3555–3560.
34. Newcomb, M., P.F. Hollenberg, and M.J. Coon (2003). Multiple mechanisms and multiple oxidants in P450-catalyzed hydroxylations. *Arch. Biochem. Biophys.* **409**, 72–79.
35. Veeger, C. (2002). Does P450-type catalysis proceed through a peroxo-iron intermediate? A review of studies with microperoxidase. *J. Inorg. Biochem.* **9**, 35–45.

36. Davydov, R., T.M. Markis, V. Kofman, D.E. Werst, S.G. Sligar, and B.M. Hoffman (2001). Hydroxylation of camphor by reduced oxy-cytochrome P-450cam: Mechanistic implications of Epr and Endor studies of catalytic intermediates in native and mutant enzymes. *J. Am. Chem. Soc.*, **123**, 1413–1415.
37. Ogliaro, F., S.P. de Visser, S. Cohen, P.K. Sharma, and S. Shaik (2002). Searching for the second oxidant in the catalytic cycle of cytochrome P450: A theoretical investigation of the iron(III)- hydroperoxo species and its epoxidation pathways. *J. Am. Chem. Soc.* **124**, 2806–2817.
38. Kamachi, T., Y. Shiota, T. Ohta, and K. Yoshizawa (2003). Does the hydroperoxo species of cytochrome P450 participate in olefin epoxidation with the main oxidant, compound I? criticism from density functional theory calculations. *Bull. Chem. Soc. Jpn.* **6**, 721–732.
39. Groves, J.T. and Y. Watanabe (1988). Reactive iron porphyrin derivatives related to the catalytic cycles of cytochrome P450 and peroxidase. Studies of the mechanism of oxygen activation. *J. Am. Chem. Soc.* **110**, 8443–8452.
40. Akhtar, M., D. Corina, S. Miller, A.Z. Shyadehi, and J.N. Wright (1994). Mechanism of the acyl-carbon cleavage and related reactions catalyzed by multifunctional P-450s: Studies on cytochrome P45017r. *Biochemistry* **33**, 4410–4418.
41. Cole, P.A. and C.H. Robinson (1988). A peroxide model reaction for placental aromatase. *J. Am. Chem. Soc.* **110**, 1284–1285.
42. Vaz, A.D.N., E.S. Roberts, and M.J. Coon (1991). Olefin formation in the oxidative deformylation of aldehydes by cytochrome P-450. Mechanistic implications for catalysis by oxygen-derived peroxide. *J. Am. Chem. Soc.* **113**, 5886–5887.
43. Sheng, D., D.P. Ballou, and V. Massey (2001). Mechanistic studies of cyclohexanone monooxygenase: Chemical properties of intermediates involved in catalysis. *Biochemistry* **40**, 11156–11167.
44. Colonna, S., N. Gaggero, G. Carrea, G. Ottolina, P. Pasta, and F. Zambianchi (2002). First asymmetric epoxidation catalysed by cyclohexanone monooxygenase. *Tetrahedron Lett.* **43**, 1797–1799.
45. Watanabe, Y. (2001). Alternatives to the oxoferryl porphyrin cation radical as the proposed reactive intermediate of cytochrome P450: Two-electron oxidized Fe(III) porphyrin derivatives. *J. Biol. Inorg. Chem.* **6**, 846–856.
46. Groves, J.T. and N. Jin (1999). Unusual kinetic stability of a ground state singlet oxomanganese(V) porphyrin. Evidence for a spin state crossing effect. *J. Am. Chem. Soc.* **121**, 2923–2924.
47. Volz, T.J., D.A. Rock, and J.P. Jones (2002). Evidence for two different active oxygen species in cytochrome P-450 BM3 mediated sulfoxidation and N-dealkylation reactions. *J. Am. Chem. Soc.* **124**, 9724–9725.
48. Nam, W., S.W. Jin, M.H. Lim, J.Y. Ryu, and C. Kim (2002). Anionic ligand effect on the nature of epoxidizing intermediates in iron porphyrin complex-catalyzed epoxidation reactions. *Inorg. Chem.* **41**, 3647–3652.
49. Machii, K., Y. Watanabe, and I. Morishima (1995). Acylperoxo-iron(III) porphyrin complexes: A new entry of potent oxidants for the alkene epoxidation. *J. Am. Chem. Soc.* **117**, 6691–6697.
50. Suzuki, N., T. Higuchi, and T. Nagano (2002). Multiple active intermediates in oxidation reaction catalyzed by synthetic heme-thiolate complex relevant to cytochrome P450. *J. Am. Chem. Soc.* **124**, 9622–9628.
51. Yoshioka, S., T. Tosha, S. Takahashi, K. Ishimori, H. Hori, and I. Morishima (2002). Roles of the proximal hydrogen bonding network in cytochrome P450cam-catalyzed oxygenation. *J. Am. Chem. Soc.* **124**, 14571–14579.
52. Manchester, J.I., J.P. Dinnocenzo, L.A. Higgins, and J.P. Jones (1997). A new mechanistic probe for cytochrome P450: An application of isotope effect profiles. *J. Am. Chem. Soc.* **119**, 5069–5070.
53. Ortiz de Montellano, P.R. and R.A. Stearns (1987). Bicyclopentane P450. *J. Am. Chem. Soc.* **109**, 3415–3420.
54. Atkinson, J.K. and K.U. Ingold (1993). Cytochrome P450 hydroxylation of hydrocarbons: Variation in the rate of oxygen rebound using cyclopropyl radical clocks including two new ultrafast probes. *Biochemistry* **32**, 9209–9214.
55. Newcomb, M. and P.H. Toy (2000). Hypersensitive radical probes and the mechanisms of cytochrome P450-catalyzed hydroxylation reactions. *Acc. Chem. Res.* **33**, 449–455.
56. Bowry, V.W. and K.U. Ingold (1991). A radical clock investigation of microsomal cytochrome P-450 hydroxylation of hydrocarbons. Rate of oxygen rebound. *J. Am. Chem. Soc.* **113**, 5699–5707.
57. Newcomb, M., R. Shen, S.-Y. Choi, P.T. Toy, P.F. Hollenberg, A.D.N. Vaz *et al.* (2000). Cytochrome P450-catalyzed hydroxylation of mechanistic probes that distinguish between radicals and cations. Evidence for cationic but not for radical intermediates. *J. Am. Chem. Soc.* **122**, 2677–2686.
58. Wüst, M. and R.B. Croteau (2002). Hydroxylation of specifically deuterated limonene enantiomers by cytochrome P450 limonene-6-hydroxylase reveals the mechanism of multiple product formation. *Biochemistry* **41**, 1820–1827.
59. Audergon, C., K.R. Iyer, J.P. Jones, J.F. Darbyshire, and W.F. Trager (1999). Experimental and theoretical study of the effect of active-site constrained

substrate motion on the magnitude of the observed intra-molecular isotope effect for the P450 101 catalyzed benzylic hydroxylation of isomeric xylenes and 4,4′-dimethylbiphenyl. *J. Am. Chem. Soc.* **121**, 41–47.

60. (a) Shaik, S., S.P. de Visser, F. Ogliaro, H. Schwarz, and D. Schröder (2002). Two-state reactivity mechanisms of hydroxylation and epoxidation by cytochrome P-450 revealed by theory. *Curr. Opin. Chem. Biol.* **6**, 556–567; (b) Sharma, P.K., S.P. de Visser, and S. Shaik (2003). Can a single oxidant with two spin states masquerade as two different oxidants? A study of the sulfoxidation mechanism by cytochrome P450. *J. Am. Chem. Soc.* **125**, 8698–8699.
61. Schröder, D., A. Fiedler, M.F. Ryan, and H. Schwarz (1994). Surprisingly low reactivity of base FeO^+ in its spin-allowed, highly exothermic reaction with molecular hydrogen to generate Fe^+ and water. *J. Phys. Chem.* **98**, 68–70.
62. Schoneboom, J.C., H. Lin, N. Reuter, W. Thiel, S. Cohen, F. Ogliaro *et al.* (2002). The elusive oxidant species of cytochrome P450 enzymes: Characterization by combined quantum mechanical/molecular mechanical (Qm/Mm) calculations. *J. Am. Chem. Soc.* **124**, 8142–8151.
63. Auclaire, K., Z. Hu, D.M. Little, P.R. Ortiz de Montellano, and J.T. Groves (2002). Revisiting the mechanism of P-450 enzymes using the radical clocks norcarane and spiro[2,5]octane, 2002. *J. Am. Chem. Soc.* **124**, 6020–6027.
64. Newcomb, M., R.N. Shen, Y. Lu, M.J. Coon, P.F. Hollenberg, D.A. Kopp *et al.* (2002). Evaluation of norcarane as a probe for radicals in cytochome P450-and soluble methane monooxygenase-catalyzed hydroxylation reactions. *J. Am. Chem. Soc.* **124**, 6879–6886.
65. Ogliaro, F., S.P. de Visser, J.T. Groves, and S. Shaik (2001). Chameleon states: High-valent metal-oxo species of cytochrome P450 and its ruthenium analog. *Angew. Chem. Int. Ed.* **40**, 2874–2878.
66. Sharma, P.K., S.P. de Visser, F. Ogliaro, and S. Shaik (2003). Is the ruthenium analogue of compound I of cytochrome P450 an efficient oxidant? A theoretical investigation of the methane hydroxylation reaction. *J. Am. Chem. Soc.* **125**, 2291–2300.
67. Kamachi, T. and K. Yoshizawa (2003). A theoretical study on the mechanism of camphor hydroxylation by compound I of cytochrome P450. *J. Am. Chem. Soc.* **125**, 4652–4661.
68. Guallar, V., M.-H. Baik, S.J. Lippard, and R.A. Friesner (2003). Peripheral heme substituents control the hydrogen-atom abstraction chemistry in cytochromes P450. *Proc. Natl. Acad. Sci., USA* **100**, 6998–7002.
69. Reyes, M.B. and B.K. Carpenter (1998). Evidence for interception of nonstatistical reactive trajectories for a singlet biradical in supercritical propane. *J. Am. Chem. Soc.* **120**, 1641–1642.
70. McMahon, R.J. (2003). Chemical reactions involving quantum tunneling. *Science* **299**, 833–834.
71. Zuev, P.S., R.S. Sheridan, T.V. Albu, D.G. Truhlar, D.A. Hrovat, and W.T. Borden (2003). Carbon tunneling from a single quantum state. *Science* **299**, 867–870.
72. Horn, A.H.C. and T. Clark (2003). Does metal ion complexation make radical clocks run fast? *J. Am. Chem. Soc.* **125**, 2809–2816.
73. Kopp, D.A. and S.J. Lippard (2002). Soluble methane monooxygenase: Activation of dioxygen and methane. *Curr. Opin. Chem. Biol.* 568–576.
74. Austin, R.N., H.-K. Chang, G.J. Zylstra, and J.T. Groves (2000). The non-heme diiron alkane monooxygenase of *Pseudomonas oleovorans* (AlkB) hydroxylates via a substrate radical intermediate. *J. Am. Chem. Soc.* **122**, 11747–11748.
75. Brazeau, B.J., R.N. Austin, C. Tarr, J.T. Groves, and J.D. Lipscomb (2001). Intermediate Q from soluble methane monooxygenase hydroxylates the mechanistic substrate probe norcarane: Evidence for a stepwise reaction. *J. Am. Chem. Soc.* **123**, 11831–11837.
76. Austin, R.N., K. Buzzi, E. Kim, G.B. Zylstra, and J.T. Groves (2003). Xylene monooxygenase, a membrane-spanning non-heme diiron enzyme that hydroxylates hydrocarbons via a substrate radical intermediate. *J. Biol. Inorg. Chem.* **8**, 733–739.
77. Wei, C.C., Z.-Q. Wang, A.L. Meade, J.F. McDonald, and D.J. Stuehr (2002). Why do nitric oxide synthases use tetrahydrobiopterin? *J. Inorg. Biochem.* **91**, 618–624.
78. Wei, C.C., Z.Q. Wang, Q. Wang, A.L. Meade, C. Hemann, R. Hille *et al.* (2001). Rapid kinetic studies link tetrahydrobiopterin radical formation to heme-dioxy reduction and arginine hydroxylation in inducible nitric-oxide synthase. *J. Biol. Chem.* **276**, 315–319.
79. Hurshman, A.R., C. Krebs, D.E. Edmondson, B.H. Huynh, and M.A. Marletta (1999). Formation of a pterin radical in the reaction of the heme domain of inducible nitric oxide synthase with oxygen. *Biochemistry* **38**, 15689–15696.
80. Hurshman, A.R. and M.A. Marletta (2002). Reactions catalyzed by the heme domain of inducible nitric oxide synthase: Evidence for the involvement of tetrahydrobiopterin in electron transfer. *Biochemistry* **41**, 3439–3456.
81. Rosen, G.M., P. Tsai, and S. Pou (2002). Mechanism of free-radical generation by nitric oxide synthase. *Chem. Rev.* **102**, 1191–1199.
82. Blasko, E., C.B. Glaser, J.J. Devlin, W. Xia, R.I. Feldman, M.A. Polokoff *et al.* (2002). Mechanistic studies with potent and selective inducible nitric-oxide synthase dimerization inhibitors. *J. Biol. Chem.* **277**, 295–302.

83. Davydov, R., A. Ledbetter-Rogers, P. Martasek, M. Larukhin, M. Sono, J.H. Dawson *et al.* (2002). Epr and endor characterization of intermediates in the cryoreduced oxy-nitric oxide synthase heme domain with bound L-arginine or N-G-hydroxyarginine. *Biochemistry* **41**, 10375–10381.
84. Huang, H., J.M. Hah, and R.B. Silverman (2001). Mechanism of nitric oxide synthase. Evidence that direct hydrogen atom abstraction from the O-H bond of N-G-hydroxyarginine is not relevant to the mechanism. *J. Am. Chem. Soc.* **123**, 2674–2676.
85. Li, H., H. Shimizu, M. Flinspach, J. Jamal, W. Yang, M. Xian *et al.* (2002). The novel binding mode of N-alkyl-N′hydroxyguanidine to neuronal nitric oxide synthase provides mechanistic insights into no biosynthesis. *Biochemistry* **41**, 13868–13875.
86. Groves, J.T. and Y.-Z. Han (1995). Models and mechanisms of cytochrome P450 action. In P.R.O.d. Montellano (ed.), *Cytochrome P-450. Structure, Mechanism and Biochemistry.* Plenum Press, New York, pp. 3–48.
87. Davies, J.A., P.L. Watson, A. Greenberg, and J.F. Liebman (1994). *Selective Hydrocarbon Activation: Principle and Progress.* VCH, New York.
88. Watanabe, Y. (1999). High valent intermediates. In K. Kadish, (ed.), *The Porphyrin Encyclopedia.* pp. 97–117.
89. Groves, J.T., T.E. Nemo, and R.S. Myers (1979). Hydroxylation and epoxidation catalyzed by iron-porphine complexes. Oxygen transfer from iodosylbenzene. *J. Am. Chem. Soc.* **101**, 1032–1033.
90. Penner-Hahn, J.E., T.J. McMurry, M. Renner, L. Latos-Grazynsky, K.S. Eble, I.M. Davis *et al.* (1983). X-ray absorption spectroscopic studies of high-valent iron porphyrins: Horseradish peroxidase (HRP) compounds I and II. *J. Biol. Chem.* **258**, 12761–12764.
91. Penner-Hahn, J.E., K.S. Eble, T.J. McMurry, M. Renner, A.L. Balch, J.T. Groves *et al.* (1986). Structural characterization of horseradish peroxidase using EXAFS spectroscopy. Evidence for Fe=O ligation in compounds I and II. *J. Am. Chem. Soc.* **108**, 7819–7825.
92. Groves, J.T., R. Quinn, T.J. McMurry, G. Lang, and B. Boso (1984). Iron(IV) porphyrins from iron(III) porphyrin cation radicals. *J. Chem. Soc. Chem. Commun.* 1455–1456.
93. Boso, B., G. Lang, T. McMurry, and J.T. Groves (1983). Mössbauer-effect study of tight spin coupling in oxidized chloro-5,10,15,20-tetra(mesityl) porphyrinatoiron(III). *J. Chem. Phys.* **79**, 1122–1126.
94. Jayaraj, K., A. Gold, R.N. Austin, L.M. Ball, J. Terner, D. Mandon *et al.* (1997). Compound I and compound II analogues from porpholactones. *Inorg. Chem.* **36**, 4555–4566.
95. Ayougou, K., D. Mandon, J. Fischer, R. Weiss, M. Muther, and V. Schunemann (1996). Molecular structure of the chloroiron(III) derivative of the meso-unsubstituted 2,7,12,17-tetramethyl-3,8,13, 18-tetramesitylporphyrin and weak ferromagnetic exchange interactions in the a(1u) oxoiron(IV) porphyrin Pi radical cation complex. *Chem. Eur. J.* **2**, 1159–1163.
96. Jayaraj, K., J. Terner, A. Gold, D.A. Roberts, R.N. Austin, D. Mandon *et al.* (1996). Influence of meso substituents on electronic states of (oxoferryl)porphyrin Pi-cation radicals. *Inorg. Chem.* **35**, 1632–1640.
97. Jayaraj, K., A. Gold, R.N. Austin, D. Mandon, R. Weiss, J. Terner *et al.* (1995). Compound-I and compound-II analogs of a chlorine. *J. Am. Chem. Soc.* **117**, 9079–9080.
98. Muther, M., E. Bill, A.X. Trautwein, D. Mandon, R. Weiss, A. Gold *et al.* (1994). Spin coupling in distorted high-valent Fe(IV) porphyrin radical complexes. *Hyperfine Interact.* **91**, 803–808.
99. Nam, W., S.K. Choi, M.H. Lim, J.U. Rohde, I. Kim, J. Kim *et al.* (2003). Reversible formation of iodosylbenzene-iron porphyrin intermediates in the reaction of oxoiron(IV) porphyrin Pi-cation radicals and iodobenzene. *Angew. Chem. Int. Ed.* **42**, 109–111.
100. Groves, J.T. and T.J. McMurry (1985). Synthetic analogs of oxidized heme proteins. Preparation and characterization of iron(IV) porphyrins. *Rev. Port. Chim.* **27**, 102–103.
101. Fujii, H., T. Yoshimura, and H. Kamada (1997). Imidazole, and *p*-nitrophenolate complexes of oxoiron(IV) porphyrin-cation radicals as models for compounds I of peroxidase and catalase. *Inorg. Chem.* **36**, 6142–6143.
102. Groves, J.T., R.C. Haushalter, M. Nakamura, T.E. Nemo, and B.J. Evans (1981). High-valent iron-porphyrin complexes related to peroxidase and cytochrome P-450. *J. Am. Chem. Soc.* **102**, 2884–2886.
103. Groves, J.T. and Y. Watanabe (1988). Reactive iron porphyrin derivatives related to the catalytic cycles of cytochrome P450 and peroxidase. Studies of the mechanism of oxygen activation. *J. Am. Chem. Soc.* **110**, 8443–8452.
104. Nam, W., Y.M. Goh, Y.J. Lee, M.H. Lim, and C. Kim (1999). Biomimetic alkane hydroxylations by an iron(III) porphyrin complex with H_2O_2 and by a high-valent iron(IV) oxo porphyrin cation radical complex. *Inorg. Chem.* **38**, 3238.
105. Gross, Z. and S.A. Nimri (1994). Pronounced axial ligand effect on the reactivity of oxoiron(IV) porphyrin cation radicals. *Inorg. Chem.* **33**, 1731–1732.
106. Gross, Z., S. Nimri, C.M. Barzilay, and L. Simkhovich (1997). Reaction profile of the last step in cytochrome P-450 catalysis revealed by studies of model complexes. *J. Biol. Inorg. Chem.* **2**, 492–506.

107. Gross, Z. and S. Ini (1997). Remarkable effects of metal, solvent and oxidant on metalloporphyrin-catalyzed enantioselective epoxidation of olefins. *J. Org. Chem.* **62**, 5514–5521.
108. Groves, J.T., Z. Gross, and M.K. Stern (1994). Preparation and reactivity of oxoiron(IV) porphyrins. *Inorg. Chem.* **33**, 5065–5072.
109. Liu, M.H. and Y.O. Su (1998). Selective electrocatalysis of alkene oxidations in aqueous media. Electrochemical and spectral characterization of oxo-ferryl porphyrin, oxo-ferryl porphyrin radical cation and their reaction products with alkenes at room temperature. *J. Electroanal. Chem.* **452**, 113–125.
110. Nam, W., H.J. Han, S.Y. Oh, Y.J. Lee, M.H. Choi, S.Y. Han *et al.* (2000). New insights into the mechanisms of O–O bond cleavage of hydrogen peroxide and tert-alkyl hydroperoxides by iron(III) porphyrin complexes. *J. Am. Chem. Soc.* **122**, 8677–8684.
111. Groves, J.T., W.J. Kruper, and R.C. Haushalter (1980). Hydrocarbon oxidations with oxometalloporphinates. Isolation and reactions of a (porphinato)manganese(V) complex. *J. Am. Chem. Soc.* **102**, 6377–6380.
112. Hill, C.L. and B.C. Schardt (1980). Alkane activation and functionalization under mild conditions by a homogeneous manganese(III)porphyrin-iodosylbenzene oxidizing system. *J. Am. Chem. Soc.* **102**, 6374–6375.
113. Meunier, B., E. Guilmet, M.E. De Carvalho, and R. Poilblanc (1984). Sodium hypochlorite: A convenient oxygen source for olefin epoxidation catalyzed by (porphyrinato)manganese complexes. *J. Am. Chem. Soc.* **106**, 6668–6676.
114. De Poorter, B. and B. Meunier (1985). Metalloporphyrin-catalyzed epoxidation of terminal olefins with hypochlorite salts or potassium hydrogen persulfate. *Perkin Trans. II, J. Chem. Soc.* 1735–1740.
115. Collman, J.P., J.I. Brauman, and B. Meunier (1984). Epoxidation of olefins by cytochrome P-450 model compounds: Mechanism of oxygen atom transfer. *Proc. Natl. Acad. Sci. USA* **81**, 3245–3248.
116. Collman, J.P., J.I. Brauman, B. Meunier, T. Hayashi, T. Kodadek, and S.A. Raybuck (1985). Epoxidation of olefins by cytochrome P-450 model compounds: Kinetics and stereochemistry of oxygen atom transfer and origin of shape selectivity. *J. Am. Chem. Soc.* **107**, 2000–2005.
117. Collman, J.P., T. Kodadek, and J.I. Brauman (1986). Oxygenation of styrene by cytochrome P-450 model systems. A mechanistic study. *J. Am. Chem. Soc.* **108**, 2588–2594.
118. Groves, J.T. and M.K. Stern (1988). Synthesis, characterization and reactivity of oxomanganese (IV) porphyrin complexes, *J. Am. Chem. Soc.* **110**, 8628–8638.
119. Collins, T.J. and S.W. Gordon-Wylie (1989). A manganese(V)-oxo complex. *J. Am. Chem. Soc.* **111**, 4511–4513.
120. Collins, T.J., R.D. Powell, C. Slebodnick, and E.S. Uffelman (1990). A water-stable manganese(V)-oxo complex: Definitive assignment of a Mn(V)=O infrared vibration. *J. Am. Chem. Soc.* **112**, 899–901.
121. MacDonnell, F.M., N.L.P. Fackler, C. Stern, and T.V. O'Halloran (1994). Air oxidation of a five-coordinate Mn(III) dimer to a high-valent oxomanganese(V) complex. *J. Am. Chem. Soc.* **116**, 7431–7432.
122. Miller, C.G., S.W. Gordon-Wylie, C.P. Horwitz, S.A. Strazisar, D.K. Periano, G.R. Clark *et al.* (1998). A method for driving O-atom transfer: Secondary ion binding to a tetraamide macrocyclic ligand. *J. Am. Chem. Soc.* **120**, 11540–11541.
123. Srinivasan, K.M., P. Michaud, and J.K. Kochi (1986). Epoxidation of olefins with cationic (salen)manganese(III) complexes. The modulation of catalytic activity by substituents. *J. Am. Chem. Soc.* **108**, 2309–2320.
124. Palucki, M.F., N.S. Finney, P.J. Pospisil, M.L. Güler, T. Ishida, and E.N. Jacobsen (1998). The mechanistic basis for electronic effects on enantioselectivity in the (salen)Mn(III)-catalyzed epoxidation reaction. *J. Am. Chem. Soc.* **120**, 948–954.
125. Feichtinger, D. and D.A. Plattner (1997). Direct proof for O=Mn-V(salen) complexes. *Angew. Chem. Int. Ed.* **36**, 1718–1719.
126. Sivasubramanian, K.V., M. Ganesan, S. Rajagopal, and R. Ramaraj (2002). Iron(III)-salen complexes as enzyme models: Mechanistic study of oxo(salen)iron complexes oxygenation of organic sulfides. *J. Org. Chem.* **67**, 1506–1514.
127. Jacobsen, E.N. (1995). Transition metal-catalyzed oxidations: asymmetric epoxidation. In G. Wilkinson, F.G.A. Stone, E.W. Abel, and L.S. Hegedus (eds), *Comprehensive Organometallic Chemistry II*, Vol. 12. Pergamon: New York.
128. (a) Katsuki, T. (1995). Catalytic asymmetric oxidations using optically-active (salen)manganese(III) complexes as catalysts. *Coord. Chem. Rev.* **140**, 189; (b) Katsuki, T. (2002). Chiral metallosalen complexes: Structures and catalyst tuning for asymmetric epoxidation and cyclopropanation. *Adv. Synth. Catal.* **344**(2), 131–147.
129. Gross, Z., G. Golubkov, and L. Simkhovich (2000). Epoxidation catalysis by a manganese corrole and isolation of an oxomanganese(V) corrole. *Angew. Chem. Int. Ed.* **39**, 4045–4047.
130. Meier-Callahan, A.E., H.B. Gray, and Z. Gross (2000). Stabilization of high-valent metals by corroles: Oxo tris(pentafluorophenyl)corrolato chromium(V). *Inorg. Chem.* **39**, 3605–3607.

131. Meier-Callahan, A.E., A.J. Di Bilio, L. Simkhovich, A. Mahammed, I. Goldberg, H.B. Gray *et al.* (2001). Chromium corroles in four oxidation states. *Inorg. Chem.* **40**, 6788–6793.
132. Mahammed, A., H.B. Gray, A.E. Meier-Callahan, and Z. Gross (2003). Aerobic oxidations catalyzed by chromium corroles. *J. Am. Chem. Soc.* **125**, 1162–1163.
133. Groves, J.T., Y. Watanabe, and T.J. McMurry (1983). Oxygen activation by metalloporphyrins—formation and decomposition of an acylperoxymanganese(III) complex. *J. Am. Chem. Soc.* **105**, 4489.
134. Groves, J.T. and M.K. Stern (1988). Synthesis, characterization and reactivity of oxomanganese(IV) porphyrin complexes. *J. Am. Chem. Soc.* **110**, 8628.
135. Groves, J.T. and Y. Watanabe (1986). Oxygen activation by metalloporphyrins related to peroxidase and cytochrome-P-450—direct observation of the O–O bond-cleavage step. *J. Am. Chem. Soc.* **108**, 7834–7836.
136. Groves, J.T. and S.S. Marla (1995). Peroxynitrite-induced DNA strand scission mediated by a manganese porphyrin. *J. Am. Chem. Soc.* **117**, 9578–9579.
137. Bernadou, J., A.-S. Fabiano, A. Robert, and B. Meunier (1994). "Redox Tautomerism" in high-valent metal-oxo-aquo complexes. Origin of the oxygen atom in epoxidation reactions catalyzed by water-soluble metalloporphyrins. *J. Am. Chem. Soc.* **116**, 9375–9376.
138. Pitie, M., J. Bernadou, and B. Meunier (1995). Oxidation at carbon-1′ of DNA deoxyriboses by the Mn-TMPyP/KHSO5 system results from a cytochrome P-450-type hydroxylation reaction. *J. Am. Chem. Soc.* **117**, 2935–2936.
139. Balahura, R.J., A. Sorokin, J. Bernadou, and B. Meunier (1997). Origin of the oxygen atom in C–H bond oxidations catalyzed by a water-soluble metalloporphyrin. *Inorg. Chem.* **36**, 3488–3492.
140. Czernuszewicz, R.S., Y.O. Su, M.K. Stern, K.A. Macor, D. Kim, J.T. Groves, and T.G. Spiro (1988). Oxomanganese(IV) porphyrins identified by resonance raman and infrared spectroscopy: Weak bonds and the stability of the half-filled T2g subshell. *J. Am. Chem. Soc.* **110**, 4158–4165.
141. Arasasingham, R.D., G.X. He, and T.C. Bruice (1993). Mechanism of manganese porphyrin-catalyzed oxidation of alkenes. Role of manganese(IV)-oxo species. *J. Am. Chem. Soc.* **115**, 7985–7991.
142. Yeh, H.C., C.H. Yu, J.S. Wang, S.T. Chen, Y.O. Su, and W.Y. Lin (2002). Stopped-flow kinetic study of the peroxidase reactions of mangano-microperoxidase-8. *J. Biol. Inorg. Chem.* **7**, 113–119.
143. Yeh, H.C., J.S. Wang, Y.O. Su, and W.Y. Lin (2001). Stopped-flow kinetic study of the h2o2 oxidation of substrates catalyzed by microperoxidase-8. *J. Biol. Inorg. Chem.* **6**, 770–777.
144. Meunier, B. and J. Bernadou (2000). Active iron-oxo, and iron-peroxo species in cytochrome P450 and peroxidases; oxo-hydroxo tautomerism with water-soluble porphyrins. In B. Meunier and Waldemar Adam (ed.). *Metal-Oxo and Metal-Peroxo Species in Catalytic Oxidations*, Vol. 97. Springer-Verlag, Berlin, pp. 1–35.
145. Jin, N., J.L. Bourassa, S.C. Tizio, and J.T. Groves (2000). Rapid, reversible oxygen atom transfer between an oxomanganese(V) porphyrin and bromide. A haloperoxidase mimic with enzymatic rates. *Angew. Chem. Int. Edit.* **39**, 3849–3851.
146. Groves, J.T., J. Lee, and S.S. Marla (1997). Detection and characterization of an oxomanganese(V) porphyrin complex by rapid-mixing stopped-flow spectrophotometry. *J. Am. Chem. Soc.* **119**, 6269–6273.
147. Nam, W., I. Kim, M.H. Lim, H.J. Choi, J.S. Lee, and H.G. Jang (2002). Isolation of an oxomanganese(V) porphyrin intermediate in the reaction of a manganese(III) porphyrin complex and H_2O_2 in aqueous solution. *Chem. Eur. J.* **8**, 2067–2071.
148. Nam, W., H.J. Lee, S.Y. Oh, C. Kim, and H.G. Jang (2000). First success of catalytic epoxidation of olefins by an electron-rich iron(III) porphyrin complex and H_2O_2: Imidazole effect on the activation of H_2O_2 by iron porphyrin complexes in aprotic solvent. *J. Inorg. Biochem.* **80**, 219–225.
149. Beckman, J.S. and W.H. Koppenol (1996). Nitric oxide, superoxide and peroxynitrite: The good, the bad and the ugly. *Am. J. Physiol.* **271**, C1424–C1437.
150. Marla, S.S., J. Lee, and J.T. Groves (1997). Peroxynitrite rapidly permeates phospholipid membranes. *Proc. Natl. Acad. Sci. USA* **94**, 14243–14248.
151. Lee, J., J.A. Hunt, and J.T. Groves (1997). Rapid decomposition of peroxynitrite by manganese porphyrin-antioxidant redox couples. *Bioorg. Med. Chem. Lett.* **7**, 2913–2918.
152. Groves, J.T. (1999). Peroxynitrite: Reactive, invasive and enigmatic. *Curr. Opin. Chem. Biol.* **3**, 226–235.
153. Lee, J., J.A. Hunt, and J.T. Groves (1998). Manganese porphyrins as redox-coupled peroxynitrite reductases. *J. Am. Chem. Soc.* **120**, 6053–6061.
154. Hunt, J.A., J. Lee, and J.T. Groves (1997). Amphiphilic peroxynitrite decomposition catalysts in liposomal assemblies. *Chem. Biol.* **4**, 845–858.
155. Stern, M.K., M.P. Jensen, and K. Kramer (1996). Peroxynitrite decomposition catalysts. *J. Am. Chem. Soc.* **118**, 8735–8736.
156. Lee, J., J.A. Hunt, and J.T. Groves (1998). Mechanisms of iron porphyrin reactions with peroxynitrite. *J. Am. Chem. Soc.* **120**, 7493–7501.

157. Shimanovich, R. and J.T. Groves (2001). Mechanisms of peroxynitrite decomposition catalyzed by fetmps, a bioactive sulfonated iron porphyrin. *Arch. Biochem. Biophys.* **387**, 307–317.
158. Szabo, C., J.G. Mabley, S.M. Moeller, R. Shimanovich, P. Pacher, L. Virag *et al.* (2002). Pathogenic role of peroxynitrite in the development of diabetes and diabetic vascular complications: Studies with FP15, a novel, potent peroxynitrite decomposition catalyst. *Mol. Med.* **8**, 571–580.
159. Collman, J.P., X. Zhang, V.J. Lee, E.S. Uffelman, and J.I. Brauman (1993). Regioselective and enantioselective epoxidation catalyzed by metalloporphyrins. *Science* **261**, 1404–1411.
160. Rose, E., A. Lecas, M. Quelquejeu, A. Kossanyi, and B. Boitrel (1998). Synthesis of biomimetic heme precursors. *Coord. Chem. Rev.* 178–180, 1407–1431.
161. Tani, F., M. Matsu-ura, S. Nakayama, and Y. Naruta (2002). Synthetic models for the active site of cytochrome P450. *Coord. Chem. Rev.* **226**, 219–226.
162. Fokin, A.A. and P.R. Schreiner (2002). Selective alkane transformations via radicals and radical cations: Insights into the activation step from experiment and theory. *Chem. Rev.* **102**, 1551–1593.
163. Breslow, R., Y. Huang, and X.J. Zhang (1997). An artificial cytochrome P450 that hydroxylates unactivated carbons with regio- and stereoselectivity and useful catalytic turnovers. *Proc. Natl. Acad. Sci.* **94**, 11156–11158.
164. (a) Breslow, R., X. Zhang, and Y. Huang (1997). Selective catalytic hydroxylation of a steroid by an artificial cytochrome P-450 enzyme. *J. Am. Chem. Soc.* **119**, 4535–4536; (b) Breslow, R., Y. Huang, and X.J. Zhang (1997). An artificial cytochrome P450 that hydroxylates unactivated carbons with regio- and stereoselectivity and useful catalytic turnovers, *Proc. Natl. Acad. Sci.* **94**, 11156–11158.
165. Groves, J.T. (1997). Artificial enzymes—the importance of being selective. *Nature* **389**, 329.
166. Collman, J.P., X. Zhang, R.T. Hembre, and J.I. Brauman (1990). Shape-selective olefin epoxidation catalyzed by manganese picnic basket porphyrins. *J. Am. Chem. Soc.* **112**, 5356–5357.
167. Collman, J.P., Z.W.A. Straumanis, M. Quelquejeu, and E. Rose (1999). An efficient catalyst for asymmetric epoxidation of terminal olefins. *J. Am. Chem. Soc.* **121**, 460–461.
168. Groves, J.T. and R.S. Myers (1983). Catalytic asymmetric epoxidation with chiral iron porphyrins. *J. Am. Chem. Soc.* **105**, 5791–5796.
169. Groves, J.T. and P. Viski (1989). Asymmetric hydroxylation by a chiral iron porphyrin. *J. Am. Chem. Soc.* **111**, 8537–8538.
170. Groves, J.T. and P. Viski (1990). Asymmetric hydroxylation, epoxidation and sulfoxidation catalyzed by vaulted binaphthyl metalloporphyrins. *J. Org. Chem.* **55**, 3628–3634.
171. Groves, J.T. and K.V. Shalyaev (1998). Paramagnetic ^{1}H-NMR relaxation probes of stereoselectivity in metalloporphyrin catalyzed olefin epoxidation. *Chirality* **10**, 106–119.
172. Nakayama, S., F. Tani, M. Matsu-ura, and Y. Naruta (2002). Cobalt "single-coronet" porphyrin bearing hydroxyl groups in its O-2 binding site as a new model for myoglobin and hemoglobin: Observation of unusually low frequency of V(O–O) in resonance raman spectrum. *Chem. Lett.* 496–497.
173. Matsui, E., Y. Naruta, F. Tani, and Y. Shimazaki (2003). An active-site model of prostaglandin H synthase: An iron "twin-coronet" porphyrin with an aryloxyl radical overhang and its catalytic oxygenation of 1,4-diene. *Angew. Chem. Int. Edit.* **42**, 2744–2747.
174. Shilov, A.E. and G.B. Shul'pin (1997). Activation of C–H bonds by metal complexes. *Chem. Rev.* **97**, 2897–2932.
175. Groves, J.T. and R. Quinn (1984). Models of oxidized heme proteins. Preparation and characterization of a trans-dioxoruthenium(VI) porphyrin complex. *Inorg. Chem.* **23**, 3844–3846.
176. Groves, J.T. and R. Quinn (1985). Aerobic epoxidation of olefins with ruthenium porphyrin catalysts. *J. Am. Chem. Soc.* **107**, 5790–5792.
177. Paeng, I.R. and K. Nakamoto (1990). Resonance raman spectra of reaction intermediates in oxidation process of ruthenium(II) and iron(II) porphyrins. *J. Am. Chem. Soc.* **112**, 3289.
178. Pronievich, L.M., I.R. Paeng, W. Lewandowski, and K. Nakamoto (1990). Vibrational spectra of dioxygen adducts and oxo complexes of ruthenium tetraphenylporphyrine (RuTPP) *J. Mol. Struct.* **219**, 335–339.
179. Han, Y.-Z. (1991). PhD Thesis, *Department of Chemistry*, Princeton University.
180. Dubourdeaux, P., M. Tavarès, A. Grand, R. Ramasseul, and J.-C. Marchon (1995). Preparation and crystal structure of trans-dihydroxo-[tetrakis(2,6-dichlorophenyl)porphinato]rutheniu m(IV) 2toluene. *Inorg. Chem. Acta* **240**, 657–660.
181. Ho, C., W.-H. Leung, and C.-M. Che (1991). Kinetics of C–H bond and alkene oxidation by trans-dioxoruthenium(VI) porphyrins. *J. Chem. Soc. Dalton. Trans.* **11**, 2933–2939.
182. (a) Lindsay-Smith, J.R. and P.R. Sleath (1982). Model systems for cytochrome P450 dependent monooxygenases 1. Oxidation of alkenes and aromatic compounds by tetraphenylporphinatoiron(III), Trans. II. *J. Chem. Soc.* 1009; (b) Prado-Manso, C.M.C., E.A. Vidoto, F.S. Vinhado, H.C. Sacco, K.J. Ciuffi, P.R. Martins *et al.* (1999). Characterization and catalytic activity of

iron(III) mono(4-N-methyl pyridyl)-tris (halophenyl) porphyrins in homogeneous and heterogeneous systems. *J. Mol. Catal. A-Chem.* **150**, 251–266.

183. Bortolini, O. and B. Meunier (1984). Enhanced selectivity by an open-well effect in a metalloporphyrin-catalyzed oxygenation reaction. *Perkin Trans. II, J. Chem. Soc.* 1967–1970.
184. Murahashi, S.-I., T. Naota, and N. Komiya (1995). Metalloporphyrin-catalyzed oxidations of alkanes with molecular oxygen in the presence of acetaldehyde. *Tetrahedron Lett.* **36**, 8059–8062.
185. Murahashi, S.-I. and N. Komiya (1998). New types of catalytic oxidations in organic synthesis. *Catal. Today* **41**, 339–349.
186. Ohkatsu, Y. and T. Osa (1977). Liquid-phase oxidation of aldehydes with metal tetra(paratolyl)porphyrins. *Bull. Chem. Soc. Jpn.* **50**, 2945.
187. Birnbaum, E.R., J.A. Labinger, J.E. Bercaw, and H.B. Gray (1998). Catalysis of aerobic olefic oxidation by a ruthenium perhaloporphyrin complex. *Inorg. Chim. Acta* **270**, 433–439.
188. Birnbaum, E.R., M.W. Grinstaff, J.A. Labinger, J.E. Bercaw, and H.B. Gray (1995). On the mechanism of catalytic alkene oxidation by molecular oxygen and halogenated iron porphyrins. *J. Mol. Catal. A: Chemical* **104**, L119–L122.
189. Grinstaff, M.W., M.G. Hill, J.A. Labinger, and H.B. Gray (1994). Mechanism of catalytic oxygenation of alkanes by halogenated iron porphyrins. *Science* **264**, 1311.
190. Groves, J.T. and J.S. Roman (1995). Nitrous oxide activation by a ruthenium porphyrin. *J. Am. Chem. Soc.* **117**, 5594–5595.
191. Banks, R.G.S., R.J. Henderson, and J.M. Pratt (1968). Reactions of gases in solution, 3. Some reactions of nitrous oxide with transition metal complexes. *J. Chem. Soc. (A)* 2886–2889.
192. (a) Bottomley, F., I.J. Lin, and M. Mukaida (1980). Reactions of dinitrogen oxide (nitrous oxide) with dicyclopentadienyltitanium complexes including a reaction in which carbon monoxide is oxidized. *J. Am. Chem. Soc.* **102**, 5238–5242; (b) Yamada, T., K. Hashimoto, Y. Kitaichi, K. Suzuki, and T. Ikeno (2001). Nitrous oxide oxidation of olefins catalyzed by ruthenium porphyrin complexes. *Chem. Lett.* **3**, 268–269.
193. Higuchi, T., H. Ohtake, and M. Hirobe (1989). Highly efficient epoxidation of olefins with pyridine N-oxides catalyzed by ruthenium porphyrins. *Tetrahedron Lett.* **30**, 6545–6548.
194. Higuchi, T., H. Ohtake, and M. Hirobe (1991). Highly efficient oxygen transfer reactions from various heteroaromatic N-oxides to olefins, alcohols and sulfides catalyzed by ruthenium porphyrins. *Tetrahedron Lett.* **32**, 7435–7438.
195. Ohtake, H., T. Higuchi, and M. Hirobe (1992). Highly efficient oxidation of alkanes and alkyl alcohols with heteroaromatic N-oxides catalyzed by ruthenium porphyrins. *J. Am. Chem. Soc.* **114**, 10660–10662.
196. Ohtake, H., T. Higuchi, and M. Hirobe (1995). The highly efficient oxidation of olefins, alcohols, sulfides and alkanes with heteroaromatic N-oxides catalyzed by ruthenium porphyrins. *Heterocycles* **40**, 867–903.
197. Nakagawa, H., T. Higuchi, K. Kikuchi, Y. Urano, and T. Nagano (1998). Selective deoxygenation of heteroaromatic N-oxides with olefins catalyzed by ruthenium porphyrin. *Chem. Pharm. Bull.* **46**, 1656–1657.
198. Ohtake, H., T. Higuchi, and M. Hirobe (1992). The selectivities and the mechanism of highly efficient epoxidation of olefins with 2,6-disubstituted pyridine N-oxides catalyzed by ruthenium porphyrin. *Tetrahedron Lett.* **33**, 2521–2524.
199. Higuchi, T. and M. Hirobe (1996). Four recent studies in cytochrome P450 modelings: A stable iron porphyrin coordinated by a thiolate ligand; a robust ruthenium porphyrin–pyridine N-oxide derivatives system; polypeptide-bound iron porphyrin; application to drug metabolism studies. *J. Mol. Catal. A: Chem.* **113**, 403–422.
200. Shingaki, T., K. Miura, T. Higuchi, M. Hirobe, and T. Nagano (1997). Regio- and stereo-selective oxidation of steroids using 2, 6-dichloropyridine N-oxide catalyzed by ruthenium porphyrins. *J. Chem. Soc., Chem. Commun.* 861–862.
201. Groves, J.T., M. Bonchio, T. Carofiglio, and K. Shalyaev (1996). Rapid catalytic oxygenation of hydrocarbons by ruthenium pentafluorophenylporphyrin complexes: Evidence for the involvement of a Ru(III) intermediate. *J. Am. Chem. Soc.* **118**, 8961–8962.
202. Groves, J.T., K.V. Shalyaev, M. Bonchio, and T. Carofiglio (1997). Rapid catalytic oxygenation of hydrocarbons with polyhalogenated ruthenium porphyrin complexes. *Stud. Surf. Sci. Catal.* **110**, 865–872.
203. James, B.R. (1986). Transition metal catalyzed oxidations. In A.E. Shilov (ed.), *Funda-mentals of Research in Homogeneous Catalysis*. Gordon Breach, New York, pp. 309–324.
204. Barley, M.H., D. Dolphin, and B.R. James (1984). Reversible intramolecular electron transfer within a ruthenium(III) porphyrin-ruthenium(II) porphyrin radical system induced by changes in axial ligation. *J. Chem. Soc., Chem. Commun.* 1499–1500.
205. Ojima, I. (ed.) (1993). *Catalytic Asymmetric Synthesis*, VCH, New York.
206. (a) Moro-oka, Y. and M. Akita (1998). Bio-inorganic approach to hydrocarbon oxidation. *Catalysis Today*

41, 327–338; (b) Zhang, R., W.Y. Yu, H.Z. Sun, W.S. Liu, and C.M. Che (2002). Stereo- and enantioselective alkene epoxidations: A comparative study of D-4-and D-2-symmetric homochiral trans-dioxoruthenium(VI) porphyrins. *Chem. Eur. J.* **8**, 2495–2507; (c) Simonneaux, G., and P. Le Maux (2002). Optically active ruthenium porphyrins: Chiral recognition and asymmetric catalysis. *Coord. Chem. Rev.* **228**, 43–60; (d) Funyu, S., T. Isobe, S. Takagi, D.A. Tryk, and H. Inoue (2003). Highly efficient and selective epoxidation of alkenes by photochemical oxygenation sensitized by a ruthenium(II) porphyrin with water as both electron and oxygen donor. *J. Am. Chem. Soc.* **125**, 5734–5740.

207. Mansuy, D. (1993). Activation of alkanes, the biomimetic approach. *Coord. Chem. Rev.* **125**, 129–141.
208. Gross, Z., S. Ini, M. Kapon, and S. Cohen (1996). First utilization of a homochiral ruthenium porphyrin as enantioselective epoxidation catalyst. *Tetrahedron Lett.* **37**, 7325–7328.
209. Lai, T.S., R. Zhang, K.K. Cheung, H.L. Kwong, and C.M. Che. Stoichiometric enantioselective alkene epoxidation with a chiral dioxoruthenium(VI) D-4-porphyrinato complex. *J. Chem. Soc., Dalton Trans.* **21**, 3559–3564.
210. Lai, T.S., H.L. Kwong, R. Zhang, and C.M. Che (1998). Aerobic enantioselective alkene epoxidation by a chiral trans-dioxo(D-4-porphyrinato) ruthenium(VI) complex. *J. Chem. Soc. Chem. Commun.* **15**, 1583–1584.
211. Berkessel, A. and M. Frauenkron (1997). Catalytic asymmetric epoxidation with a chiral ruthenium porphyrin and N-oxides. *J. Chem. Soc., Perkin Trans.* **16**(1), 2265–2266.